

## THE LOS ARCHIPELAGO NEPHELINE SYENITE RING-STRUCTURE: A MAGMATIC MARKER OF THE EVOLUTION OF THE CENTRAL AND EQUATORIAL ATLANTIC

CHRISTIAN MOREAU

*Département des Sciences de la Terre et CNRS – URA10, Pôle Sciences et Technologie,  
Université de La Rochelle, Avenue Marillac, 17042 La Rochelle Cedex 1, France*

DANIEL OHNENSTETTER

*Centre de Recherche Pétrographiques et Géochimiques – Centre National de la Recherche Scientifique,  
B.P. 20, 54501 Vandoeuvre-lès-Nancy Cedex, France*

DANIEL DEMAIFFE

*Département des Sciences de la Terre, C.P. 160/02, Université Libre de Bruxelles,  
50, avenue F.D. Roosevelt, 1050 Bruxelles, Belgique*

BERNARD ROBINEAU

*Département des Sciences de la Terre, Université de la Réunion,  
15, avenue René Cassin, 97489 Saint-Denis Cedex, La Réunion*

### ABSTRACT

The Los Archipelago ring structure (Guinea, West Africa) is composed of peralkaline nepheline syenite, which crops out over two long crescent-shaped islands (Tamara, Kassa), five islets and a central island (Roume). A detailed geological study, which led to a new geological map, recognizes several series within two main petrographic suites, on the basis of textural and structural field criteria. The first suite is miaskitic and is composed of hastingsite-augite nepheline syenite, whereas the second suite is agpaitic and is mainly composed of arfvedsonite-aegirine nepheline syenite. These formations are intruded by microsyenite of the same composition and then by ring-shaped monchiquitic and radial phonolitic dykes. Late pegmatites cross-cut all the rocks. A Rb-Sr whole-rock isochron gives an age of  $104.3 \pm 1.7$  ( $2\sigma$ ) Ma (MSWD = 1.28). The initial Sr isotopic composition ( $^{87}\text{Sr}/^{86}\text{Sr}_0 = 0.7040$ ) is compatible with a mantle origin with minor or no crustal influence. The geological environment and the emplacement age of the Los Archipelago point to formation during the continental breakup between the West Africa and South America and early rifting of the Equatorial Atlantic Ocean.

**Keywords:** miaskitic nepheline syenite, agpaitic nepheline syenite, Rb-Sr geochronology, continental breakup, Equatorial Atlantic Ocean, Los Archipelago, Guinea.

### SOMMAIRE

L'archipel de Los (Guinée, Afrique de l'Ouest), est un complexe annulaire composé de syénite néphelinique hyperalcaline affleurant sur deux îles en forme de croissant (Tamara et Kassa), cinq îlots et l'île centrale de Roume. Une étude géologique détaillée a permis d'établir une nouvelle carte géologique où l'on a distingué au sein de deux grandes suites de syénite néphelinique plusieurs séries selon des critères texturaux et structuraux établis sur le terrain. La première suite, miaskitique, est composée essentiellement de syénite néphelinique à hastingsite et augite. La seconde suite, agpaitique, est constituée de syénite néphelinique à aegirine et arfvedsonite. L'ensemble de ces syénites est injecté par des venues de microsyénite de même composition, puis traversé par des filons annulaires de monchiquite et radiaires de phonolite. Des filons de pegmatite tardive recoupent l'ensemble des formations de la structure. Une isochrone Rb-Sr sur roche totale a donné un âge de  $104.3 \pm 1.7$  ( $2\sigma$ ) Ma (MSWD = 1.28) pour l'ensemble des formations syénitiques. Le rapport isotopique initial ( $^{87}\text{Sr}/^{86}\text{Sr}_0$ ), égal à 0.7040, est compatible avec une source mantellique légèrement appauvrie, sans (ou avec peu) d'influence crustale. L'environnement géologique et l'âge de mise en place de l'archipel de Los permettent de le considérer comme un bon marqueur magmatique intervenu lors du changement de régime tectonique, correspondant à la séparation de l'Afrique de l'Ouest et de l'Amérique du Sud et donnant naissance à l'Océan Atlantique Equatorial.

**Mots-clés:** syénite néphelinique miaskitique, syénite néphelinique agpaitique, datation Rb-Sr, séparation des continents, océan Atlantique équatorial, archipel de Los, Guinée.

## INTRODUCTION

The Los Archipelago ( $9^{\circ}30'N$ ,  $15^{\circ}30'E$ ), located 5 km offshore Conakry (Guinea, western Africa), is composed of two long crescent-shaped islands (Kassa and Tamara) and five islets (Corail, Blanche, Cabri, Fousset and Poulet) that encircle an internal lagoon and its central island, Rourne (Figs. 1, 2). This nepheline syenite complex was studied by Gürich (1887), Lacroix (1911), Delaire & Renaud (1955), Lazarenkov (1975) and Moreau *et al.* (1986). The circular shape of the archipelago was first commented upon by Millot & Dars (1959), who interpreted the islands as the expression of a ring structure comparable to those observed in Cameroon, Nigeria, Madagascar, South Africa and western Africa. Moreau *et al.* (1986) emphasized the importance of the magmatic structures in the syenites and described the xenoliths, dykes, and veins. In terms

of size (12 km in diameter,  $115 \text{ km}^2$ ), petrology and high level of emplacement, the Los complex is similar to the Ilímaussaq massif ( $100 \text{ km}^2$ ) in Greenland (Upton 1974, Larsen & Sørensen 1987), but smaller than the Khibina–Lóvozero pluton ( $2000 \text{ km}^2$ ) in the Kola peninsula (Dudkin & Mitrofanov 1994, Semenov 1994).

Most of the anorogenic ring-structures intrude either a continental intraplate environment, such as in the Air, Nigeria and Cameroon provinces, or an oceanic intraplate environment, such as at Kerguelen Island (Black *et al.* 1985). In contrast, the Los complex intrudes a passive continental margin; it thus bears some resemblance to the Canary and Cape Verde complexes (Crévolá *et al.* 1994), which also intrude the passive margin of west Africa, and the Trindade and Fernando do Noronha intrusions, located on the Brazilian passive margin (Ulrich & Gomes 1981).

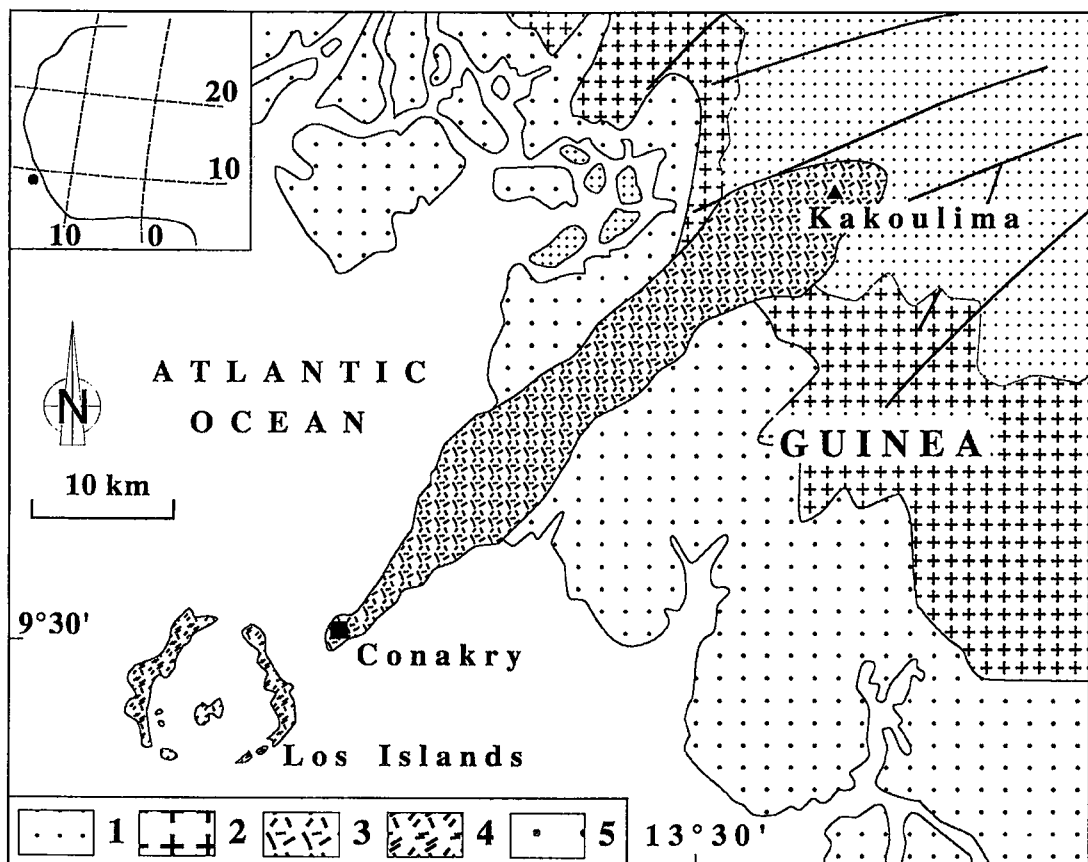


FIG. 1. Geological sketch map showing the location of the Los Islands (Millot & Dars 1959) in the prolongation of the Conakry Peninsula. Insert: location of the studied area in West Africa. 1: Paleozoic white sandstone of the Bove basin; 2: Proterozoic calc-alkaline porphyritic biotite granite; 3: Kakoulima gabbro and peridotite; 4: Los Islands nepheline syenite; 5: marine alluvium.

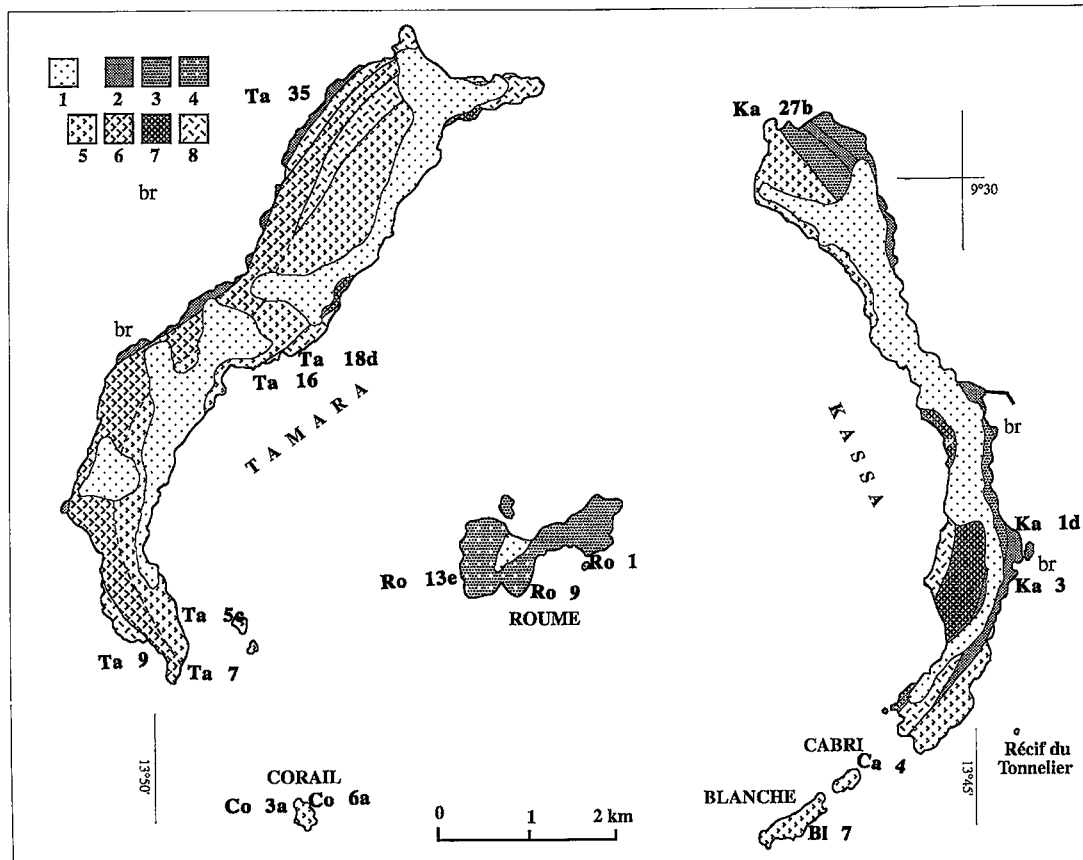


FIG. 2. Geological map of Los Archipelago. 1: bauxitic laterite. *Agpaitic suite* (aegirine – arfvedsonite – lâvenite – kupletsksite nepheline syenite); 2: fine-grained and microcrystalline type; 3: medium- to coarse-grained type; 4: brecciated type. *Miaskitic suite* (hastingsite – augite nepheline syenite); 5: medium- to coarse-grained type; 6: “nebulous” type; 7: mesocratic type; 8: leucocratic type; br: occurrence of endogenous breccia.

A new 1:50 000 map of the complex (Fig. 2), completed as a result of a detailed structural and petrological study (Moreau *et al.* 1986), shows that the main rock-types pass gradationally from one to the other; sharp contacts are completely lacking, which points to a single phase of intrusion. Detailed mineralogical, petrological and geochemical data have been obtained on the main rock-types of the Los complex. An Rb–Sr whole-rock isochron allows us to place the Los archipelago magmatic event temporally in relation to the evolution of the Central and Equatorial Atlantic Ocean. A new interpretation of the emplacement of this complex in its geodynamic environment is presented.

#### GEOLOGICAL SETTING

From the geodynamic point of view, the Los complex intrudes a passive continental margin made of early Mesozoic continental platform sediments that overlie a Proterozoic basement (Villeneuve 1984).

The Los intrusive complex was emplaced during the Cretaceous, at the western edge of the Conakry Peninsula, consisting essentially of the elongate (50 km) Kaloum ultramafic body. The eastern part of this complex, known as the Kakoulima massif, is made of a thick sequence of layered peridotite and gabbro, of tholeiitic affinity, forming a huge laccolith (Delaire & Renaud 1955, Barrère 1959, Diallo *et al.* 1992) that intruded the West African Proterozoic basement and the Paleozoic sediments of the Bove basin (Fig. 1). The Freetown layered complex (Sierra Leone), dated at  $193 \pm 3$  Ma (Rb–Sr age: Beckinsale *et al.* 1977), is similar to the Kakoulima massif. These intrusions have been related to the formation of the Central Atlantic passive margin (Diallo *et al.* 1992). There is, however, no direct field relation between the Kaloum–Kakoulima tholeiitic intrusive complex and the Los silica-under-saturated alkaline suite. In particular, there is no evidence that the younger Los complex cross-cuts the tholeiitic stratiform complex at depth.

## FIELD RELATIONSHIPS AND PETROGRAPHY

Two main petrographic suites have been described in the Los Islands, a miaskitic one, and the other agpaitic (Fig. 2) (Lacroix 1911, Delaire & Renaud 1955, Moreau *et al.* 1986). The distinction between agpaitic and miaskitic suites is classically done on the basis of mineralogical composition (Sørensen 1974). Xenoliths, veins and dyke rocks cutting the complex are grouped into families (phonolite, microshonkinite, and monchiquite) on the basis of their petrography.

Detailed field and structural studies of the whole Los intrusive complex (Moreau *et al.* 1986) suggest four stages of emplacement: 1) the agpaitic and miaskitic nepheline syenite – microsyenite, forming the largest part of the complex, were emplaced together at an early stage; 2) the nepheline microsyenite and aplite were emplaced later, followed by 3) ring dykes (and endogenous breccias) and, finally, 4) radial dykes and late pegmatites. The general shape of the whole complex and its internal structures correspond to those of a lopolith. The center of igneous activity seems to be located on Roume Island, where a widespread endogenous breccia is found. There is no evidence for the possible existence of two centers.

### *Agpaitic syenite*

Agpaitic syenite cover only one quarter of the surface at Los. Such rocks contain lävenite- and astrophyllite-group minerals (Gürich 1887) and rare minerals such as villiaumite (Lacroix 1908), serandite (Lacroix 1931) and steacyite (Parodi & Della Ventura 1987). The texture is foyaitic to locally trachytoid, as a result of flow of the syenitic magma during its emplacement. A transition toward a microcrystalline texture has been noted, as well as toward a pegmatitic facies. Mineralized druses occur, especially on Roume Island and in a quarry at the north of Kassa.

A detailed survey permits to distinguish three different types. 1) A coarse- to medium-grained aegirine nepheline syenite shows an intergranular foyaitic texture, as in the external rim (Fig. 2) of some islands (northeast of Kassa: Ka 27b, Ka 1d; northwest of Tamara: Ta 35) and in the center of the structure at Roume Island (Ro 1, Ro 9). This syenite is composed of euhedral laths of perthitic feldspar, commonly mantled by albite, and interstitial, anhedral feldspathoids (nepheline, sodalite, and analcime), associated with poikilitic Mn-rich arfvedsonite. Euhedral and zoned crystals of lävenite, kupletskite, and aegirine are associated with small crystals of pyrophanite, rare pyrochlore, with small hexagonal crystals of catapleite and fluorite in the interstices. 2) An aegirine – lävenite – nepheline microsyenite with rare kupletskite shows a microcrystalline foyaitic texture, locally with well-developed trachytic fluidal features.

The nepheline microsyenite is locally porphyritic, with alkali feldspar phenocrysts. This rock type is found mostly on the external part of the complex, along the western coast of Tamara and eastern coast of Kassa. 3) A brecciated nepheline syenite has been observed on Roume Island, locally on the southeastern part of Tamara, and on the external parts of Kassa and Tamara.

Note that the transition between agpaitic and miaskitic syenites is progressive; it has been observed in Tamara (Ta 35), Corail (Co 6a), Cabri and Blanche (Bl 7).

### *Miaskitic syenite*

Miaskitic syenite occupies the outer rim of the structure (Fig. 2), the main part of the islands of Kassa (Ka 3) and Tamara (Ta 16, Ta 7). Such rocks display a coarse-grained intersertal texture, with euhedral to subhedral alkali feldspar, and nepheline and analcime within the interstices. Augite commonly is included within the poikilitic hastingsite and is associated with euhedral crystals of titanite, apatite and titaniferous magnetite.

At the scale of the map (Fig. 2), the following petrographic types have been distinguished: 1) a mesocratic medium- to coarse-grained nepheline syenite represents the main type; it displays an intergranular to intersertal texture with local feldspathic intergrowths and mosaic concentrations of hastingsite, titanite, and augite; 2) a "nebulous" type of nepheline syenite, characterized by dark grey spotted polycrystalline aggregates of nepheline; 3) a mesocratic nepheline microsyenite, characterized by a slightly porphyritic heteromicrogranular texture; such rocks outcrop mainly as narrow bands (a few decimeters) in the northeastern and northwestern parts of Tamara and along the western coast of Kassa, and 4) a leucocratic type occurs as a light grey, feldspar- and nepheline-rich, medium to coarse-grained rock, locally with a pegmatitic (south of Kassa) or a microcrystalline texture (eastern and northeastern coast of Tamara).

### *The dykes, xenoliths and pegmatites*

Two types of dykes have been distinguished. 1) Ring dykes (decimeter to meter thick) with low inward dip. They consist mainly of phonolite. They are centered on Roume Island, but also crop out on Tamara, Kassa and Corail islands. The phonolite dykes present either a porphyritic texture or a fluidal pilotaxitic texture. The porphyritic texture (Ta 9) is defined by sanidine phenocrysts in a groundmass composed of spherulites with radial intergrowths of alkali feldspar and aegirine needles, associated with nosean, nepheline and biotite. The fluidal pilotaxitic texture (Ca 4) is composed of needles of aegirine, sanidine microphenocrysts that outline a flow-induced

lamination, and microlites in a nepheline- and analcime-rich groundmass with rare crystals of fluorite. 2) Radial dykes (centimeter to decimeter thick) are homogeneously distributed throughout the intrusive complex. They consist mainly of monchiquite and shonkinite. The monchiquite dyke from Roume Island (Ro 13e) shows an intersertal texture: zoned titaniferous augite and hastingsite phenocrysts locally occur as glomeroporphyritic clusters in a groundmass composed of intersertal alkali feldspar and microlites of titaniferous augite. Hastingsite, apatite, and titaniferous magnetite, analcime, and nepheline fill the interstices; calcite occurs as a secondary mineral. The microshonkinite dyke (Ta 18d) is a medium-grained porphyritic rock with an intersertal texture. The phenocrysts are titaniferous augite and olivine (replaced by a smectite-group mineral). The alkali feldspar laths define an intersertal texture; microlites of titaniferous augite, hastingsite, biotite, and apatite occur within an analcime- and nepheline-rich groundmass.

Magmatic xenoliths are common, but represent less than 1 vol.%; they are mainly found in miaskitic syenite. They vary in size from a few centimeters to several decimeters, and are usually ovoid, round or ellipsoidal. Two main types have been identified: 1) leucocratic xenoliths of nepheline microsyenite composition, and 2) mafic xenoliths of basanitic composition, located only in the southern part of Tamara Island (Ta 5c). On Coral Island, a large screen ( $50 \times 2$  m) of micro-essexite (Co 3a) occurs within the syenite. It contains syenitic xenoliths and is cross-cut by pegmatitic syenitic veins. A phonolitic dyke cuts all the rocks.

A basanite enclave from Tamara Island (Ta 5c) shows an intersertal texture with olivine ( $Fo_{68-44}$ ) phenocrysts, and plagioclase, augite, and hastingsite microlites, euhedral titaniferous magnetite, analcime

and apatite. The micro-essexite screen (Co 3a) from Coral Island shows a microheterograngular texture, with zoned and resorbed phenocrysts of augite, anhedral alkali feldspar associated with augite and hastingsite microlites, titaniferous magnetite, and apatite, with interstitial nepheline and analcime in the groundmass.

Dykes of pegmatite are ubiquitous; they are related to the main agpaitic and miaskitic nepheline syenites, but they are also associated with various dykes and cut some of them (Moreau *et al.* 1986).

#### ANALYTICAL METHODS

Concentrations of major and trace elements in whole rocks were determined by inductively coupled plasma (ICP) – atomic emission spectrometry at the University of Clermont-Ferrand II (Cantagrel & Pin 1994). The FeO content was established by wet chemistry at the University of Nancy I. Analyses of the minerals were obtained with a Camebax Microbeam and SX 50 electron microprobes with wavelength-dispersion spectrometers at the joint CNRS–BRGM facility. Operating conditions were: accelerating voltage 15 kV and beam current 10 nA; counting times were 10 s for major elements and 20 s for minor elements. Oxides and natural silicates were used as standards. Data reduction for the microbeam analyses was performed using the ZAF method of Henoc & Tong (1978) and, for the SX 50, using the PAP method of Pouchou & Pichoir (1984, 1991).

Isotopic analyses were carried out at the Laboratoire de Pétrologie – Géodynamique chimique of the Université Libre de Bruxelles. The samples were processed following standard chemical procedures (*i.e.*, HF– $HClO_4$  dissolution and separation using an anion-exchange column). The isotopic composition of Sr was measured on double Re filaments with a

TABLE 1. MINERALOGICAL COMPOSITION OF SELECTED SAMPLES FROM THE LOS ARCHIPELAGO

N°	Samples	Rock-type	Feld.	Foid	Ol.	Augite	Aeg.	Hast.	Arf.	Låv.	Kupl.	Mica	Ilm.	Timgt.	Eud.	Cat.	Fluo.	Tit.	Pyro.	Ap.
1	Ka 27b	agpaitic syenite	+		N, A, S		+		+	+						+	+	+	+	+
2	Ro 9	agpaitic syenite	+		N, A, S		+		+	+	+						+		+	+
3	Ta 1	agpaitic syenite	+		N, A, S		+		+	+	+						+			
4	Ka 1d	agpaitic syenite	+		N, A, S		+		+	+	+						+	+		
5	Ta 35	agpaitic syenite	+		N, A		+		+			+					+	+	+	+
6	Bl 7	miaskitic syenite	+		N,A					+		+					+			
7	Ta 18	miaskitic syenite	+		N, A, S		+		+							+				
8	Ku 3	miaskitic syenite	+		N, A		+		+							+				
9	Ta 7	miaskitic syenite	+		N, A, S		+		+			+				+				
10	Co 6a	miaskitic syenite	+		N, A		+		+							+				
11	Ta 9	phonolite	+		N, A, S		+		+								+			
12	Ca 4	phonolite	+		N, A, S		+		+										+	
13	Ro 13e	monchiquite	+		N, A		+		+			+				+				
14	Ta 18d	micro-shonkinite	+		N, A	+	+		+			+				+				
15	Co 3a	micro-essexite	+		N, A		+		+			+				+				
16	Ta 5c	basanite	+		A	+	+		+			+				+				

Feld.: feldspar; Foid: N: nepheline, A: analcime, S: sodalite; Ol: olivine; Aeg: aegirine; Hast.: hastingsite; Arf.: arfvedsonite; Låv.: lävenite; Kupl.: kupletsksite; Ilm.: ilmenite; Timgt.: titaniferous magnetite; Eud.: euclayite; Cat.: catapleite; Fluo.: fluorite; Tit.: titanite; Pyro.: pyrochlore; Ap.: apatite.

Finnigan MAT 260 mass spectrometer. Between-run precision is better than  $5 \times 10^{-5}$ . The NBS 987 standard gave a value for  $^{87}\text{Sr}/^{86}\text{Sr}$  of  $0.71023 \pm 1$  ( $2\sigma$  on the mean for 30 measurements, normalized to  $^{86}\text{Sr}/^{88}\text{Sr} = 0.1198$ ). Rb and Sr concentrations have been measured by X-ray fluorescence or by isotope dilution ( $^{87}\text{Rb}$  and  $^{84}\text{Sr}$  spike) where concentrations were less than 30 ppm. The error on the Rb/Sr ratio is  $\leq 2\%$ . The Rb/Sr age has been calculated following Williamson (1968), with an assigned error of 2% on the  $^{87}\text{Rb}/^{86}\text{Sr}$  ratios and of  $4 \times 10^{-5}$  (average between-run error) on the  $^{87}\text{Sr}/^{86}\text{Sr}$  ratios, except where the isotopic measurement for a sample was less precise.

### MINERALOGY

The petrographic features and mineral associations of the analyzed samples are summarized in Table 1. The two main suites are distinguished by mineralogy and crystal chemistry. The agpaitic syenites invariably contain aegirine, arfvedsonite commonly very much enriched in Mn (up to 9.2 wt% MnO), Mn-rich mica (up to 6.8 wt% MnO), pyrophanite, and Mn-bearing minerals such as kupletskeite and lâvenite. Villiaumite, serandite, steacyite, and phases rich in rare-earth-elements (REE) and Zr, such as eudialyte, catapleiite, rosenbuschite and pyrochlore, also characterize the agpaitic rocks. The miaskitic syenites are mineralogically characterized by hastingsitic amphibole, with lower Mn content (up to 3.9 wt% MnO), Mn-bearing mica, and an abundance of titanite. The transition between the two main suites is marked in some

samples (Ta 35 and Bl 7) by intermediate features, such as the presence of lâvenite instead of titanite. The evolution from the miaskitic to the agpaitic facies is marked by the disappearance of titanite, augite, hastingsite, and titaniferous magnetite, whose roles are played by the kupletskeite-lâvenite association, aegirine, arfvedsonite, and pyrophanite, respectively.

The composition of the pyroxenes, calculated on the basis of four cations and six atoms of oxygen (Table 2), evolves from augite in the miaskitic suite to aegirine-augite and aegirine in the agpaitic suite. In some rocks, aegirine-augite occurs as a relict core within aegirine. The prismatic crystals of aegirine commonly show oscillatory zoning. The concentration of zirconium ( $\text{ZrO}_2$  may reach 1.73 wt%) and comparable to that in the Ilmaussaq suite (Shearer & Larsen 1994). The concentration of manganese is high in both quadrilateral and Na-pyroxenes (nomenclature according to the IMA recommendations: Morimoto 1988), with MnO content up to 4.70 wt%; thus in most cases the pyroxene could be called manganoan aegirine, manganoan aegirine-augite and manganoan augite. Only a few alkaline intrusive complexes are known to contain pyroxene as Mn-rich as the Los manganoan aegirine (*i.e.*, Kangerdlugssuaq: Kempe & Deer 1970, Layne *et al.* 1982). Compared to the crystallization trends of sodium-rich pyroxenes from the literature (Fig. 3), the compositional trend at Los is close to the Ilmaussaq trend (Larsen 1976) for aegirine-rich pyroxene, and close to the Uganda (Tyler & King 1967) and South Qôroq (Stephenson 1972) trends for the quadrilateral

TABLE 2. RESULTS OF ELECTRON-MICROPROBE ANALYSES  
OF REPRESENTATIVE PYROXENES FROM THE LOS ARCHIPELAGO

sample	Ka27b 1	Ka27b 2	Rg9 3	R9/2 4	R9/5 5	Ro1 6	Ka1d 7	Ta235 8	Ro1 9	Ta16 10	Ta16 11	Cofa 12	Cofa 13	Cofa 14
SiO <sub>2</sub>	52.16	51.02	51.79	51.39	51.21	51.38	51.54	50.46	50.85	49.90	48.69	48.67	49.45	48.46
TiO <sub>2</sub>	1.14	1.29	0.49	0.39	2.11	0.96	0.35	0.09	1.50	0.46	0.41	1.22	0.86	1.01
Al <sub>2</sub> O <sub>3</sub>	1.00	0.90	0.91	0.77	1.50	0.88	1.07	0.39	0.57	2.05	1.65	2.51	2.41	2.70
Fe <sub>2</sub> O <sub>3</sub> calc.	30.63	23.72	27.90	26.45	27.68	27.27	31.67	29.41	21.90	4.26	7.34	6.86	6.47	8.11
FeO calc.	0.83	4.70	2.98	1.41	1.46	3.29	0.4	0.68	5.37	11.37	11.09	6.77	6.48	7.49
MnO	0.57	1.91	1.43	3.65	1.51	1.73	0.65	2.06	3.28	3.72	4.70	2.44	2.46	2.26
MgO	0.24	0.32	0.27	0.34	0.32	0.17	0.20	0.50	0.18	6.88	4.52	8.93	8.87	7.89
CaO	0.40	2.62	2.09	3.95	0.71	2.14	0.73	2.11	5.35	18.87	17.65	19.41	19.45	18.92
NiO	13.23	11.31	11.89	11.04	12.77	11.89	12.87	11.86	10.25	1.87	2.60	2.01	2.20	2.32
K <sub>2</sub> O	0.00	0.00	0.00	0.01	0.01	0.02	0.01	0.02	0.01	0.00	0.02	0.00	0.00	0.00
ZrO <sub>2</sub>	0.46	1.09	0.55	0.35	1.00	0.56	0.22	1.73	0.69	0.26	0.11	0.06	0.23	0.00
Nb <sub>2</sub> O <sub>5</sub>	0.00	0.10	0.00	0.00	0.00	0.38	0.00	0.00	0.52	0.00	0.00	0.00	0.00	0.00
Total	100.64	98.97	100.29	99.74	100.29	100.65	99.70	99.30	100.46	99.64	98.78	98.88	98.87	99.16
Si	1.986	1.996	1.994	1.994	1.962	1.976	1.983	1.973	1.975	1.943	1.938	1.882	1.909	1.878
Al IV	0.014	0.004	0.006	0.006	0.038	0.024	0.017	0.018	0.025	0.057	0.062	0.114	0.091	0.122
Al VI	0.031	0.037	0.035	0.029	0.030	0.016	0.032	0.000	0.001	0.037	0.016	0.000	0.018	0.001
Ti	0.033	0.038	0.014	0.011	0.061	0.028	0.010	0.002	0.044	0.013	0.012	0.036	0.025	0.029
Fe <sub>3+</sub>	0.877	0.698	0.809	0.772	0.798	0.789	0.917	0.865	0.640	0.125	0.220	0.200	0.188	0.237
Fe <sub>2+</sub>	0.026	0.154	0.096	0.046	0.047	0.106	0.013	0.022	0.174	0.370	0.369	0.219	0.209	0.243
Mn	0.018	0.063	0.047	0.120	0.049	0.056	0.021	0.068	0.104	0.123	0.158	0.008	0.080	0.074
Mg	0.014	0.19	0.015	0.020	0.018	0.009	0.011	0.029	0.011	0.399	0.268	0.515	0.510	0.456
Ca	0.016	0.110	0.085	0.164	0.029	0.088	0.030	0.089	0.223	0.787	0.753	0.804	0.804	0.785
Na	0.76	0.838	0.888	0.831	0.949	0.896	0.950	0.899	0.772	0.141	0.201	0.100	0.165	0.175
K	0.000	0.000	0.000	0.000	0.001	0.001	0.001	0.000	0.000	0.001	0.000	0.000	0.000	0.000
Zr	0.009	0.021	0.010	0.007	0.019	0.010	0.004	0.033	0.013	0.003	0.002	0.001	0.000	0.000
Nb	0.000	0.003	0.000	0.000	0.000	0.010	0.000	0.000	0.014	0.000	0.000	0.000	0.000	0.000

Columns 1 to 8: Na pyroxene; column 9: Ca-Na pyroxene; column 10 to 14: Quad pyroxene. Compositions expressed in wt%.

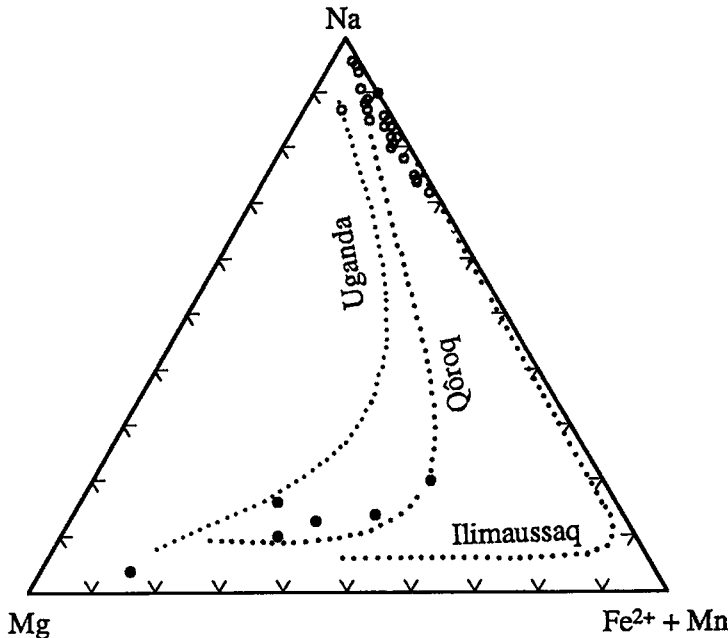


FIG. 3. Na - Mg - Fe<sup>2+</sup> + Mn triangular plot showing the Los suite of pyroxene compositions. Dots: miaskitic suite; open circles: agpaitic suite. The Ilimaussaq (Larsen 1976), South Qôroq suite (Stephenson 1972), and Uganda (Tyler & King 1967) trends also are reported.

TABLE 3. RESULTS OF ELECTRON-MICROPROBE ANALYSES  
OF REPRESENTATIVE AMPHIBOLES FROM THE LOS ARCHIPELAGO

Sample n°	Ro9 1	Ro9 2	Ro9 3	Ro1 4	Kald 5	Th35 6	Ta16 7	Ta16 8	Ka3 9	Ta7 10	Ta7 11	Ta7 12
SiO <sub>2</sub>	51.27	49.50	49.88	45.04	46.18	48.65	40.30	40.23	37.67	39.99	39.06	39.41
TiO <sub>2</sub>	0.35	0.69	0.46	2.19	1.31	0.99	3.11	2.61	1.11	3.17	1.56	1.63
Al <sub>2</sub> O <sub>3</sub>	1.38	1.63	1.43	3.92	3.81	3.09	10.95	10.14	14.07	10.58	11.04	10.86
Fe <sub>2</sub> O <sub>3</sub> calc.	2.54	4.25	3.83	7.18	8.09	6.57	5.12	5.08	6.73	1.73	4.02	6.61
Fe/O calc.	16.66	18.95	17.99	20.37	15.21	13.75	12.88	13.29	13.49	13.94	16.50	13.73
MnO	9.17	7.69	8.92	5.67	8.56	5.12	2.70	3.13	3.86	2.36	3.13	3.24
MgO	3.72	2.60	2.64	1.63	2.35	7.01	8.87	8.43	6.08	9.91	6.50	7.30
CaO	0.59	0.55	0.67	1.41	0.62	1.63	10.08	10.06	10.48	10.82	10.22	9.92
Na <sub>2</sub> O	8.19	8.29	8.16	8.24	8.54	8.62	3.16	3.00	2.74	3.19	3.08	3.10
K <sub>2</sub> O	2.25	2.13	2.19	1.68	1.62	1.57	1.60	1.68	1.91	1.68	1.86	1.71
ZrO <sub>2</sub>	0.10	0.16	0.30	0.20	0.44	0.27	0.05	0.08	0.00	0.29	0.20	0.00
F	1.79	1.26	1.25	0.59	1.55	1.45	1.99	2.61	1.42	2.35	2.06	1.83
Cl	0.00	0.02	0.00	0.01	0.00	0.00	0.03	0.00	0.00	0.04	0.03	0.02
H <sub>2</sub> O calc.	1.05	1.28	1.29	1.59	1.14	1.26	1.03	0.71	1.26	0.83	0.92	1.06
-O=F	-0.75	-0.53	-0.53	-0.25	-0.65	-0.61	-0.84	-1.10	-0.60	-0.99	-0.87	-0.77
-O=Cl	0.00	0.00	0.00	0.00	0.00	0.00	-0.01	0.00	0.00	-0.01	-0.01	0.00
Total	98.31	98.47	98.48	99.47	98.77	99.37	101.02	99.95	100.22	99.88	99.30	99.65
Si	8.092	7.902	7.958	7.222	7.372	7.494	6.114	6.201	5.846	6.137	6.154	6.135
Al iv	0.000	0.098	0.042	0.778	0.628	0.506	1.886	1.799	2.154	1.863	1.846	1.865
Al vi	0.257	0.209	0.228	0.000	0.089	0.054	0.072	0.043	0.419	0.050	0.205	0.127
Ti	0.041	0.082	0.055	0.263	0.157	0.114	0.354	0.303	0.130	0.366	0.185	0.191
Zr	0.008	0.012	0.023	0.015	0.034	0.020	0.003	0.006	0.000	0.022	0.015	0.000
Fe <sup>3+</sup>	0.302	0.510	0.460	0.867	0.973	0.762	0.584	0.589	0.786	0.200	0.477	0.774
Fe <sup>2+</sup>	2.199	2.530	2.401	2.732	2.031	1.772	1.635	1.714	1.751	1.789	2.174	1.787
Mn	1.226	1.039	1.206	0.77	1.157	0.667	0.346	0.409	0.507	0.307	0.417	0.427
Mg	0.875	0.618	0.628	0.388	0.56	1.610	2.005	1.937	1.406	2.267	1.527	1.694
Ca	0.099	0.093	0.115	0.241	0.106	0.269	1.638	1.661	1.743	1.779	1.725	1.654
Na	2.507	2.567	2.522	2.562	2.644	2.573	0.929	0.896	0.823	0.950	0.941	0.935
K	0.454	0.434	0.445	0.345	0.329	0.309	0.330	0.379	0.329	0.373	0.373	0.340
F	0.891	0.636	0.632	0.299	0.781	0.706	0.955	1.271	0.698	1.141	1.028	0.899
Cl	0.000	0.004	0.000	0.004	0.000	0.001	0.007	0.001	0.000	0.009	0.009	0.004
OH	1.109	1.360	1.368	1.698	1.219	1.293	1.038	0.728	1.302	0.85	0.963	1.096
Total	18.06	18.096	18.083	18.184	18.080	18.150	17.875	17.888	17.944	18.059	18.039	17.928

Columns 1 to 6: arfvedsonite; columns 7 to 12: hastingsite. Compositions expressed in wt%.

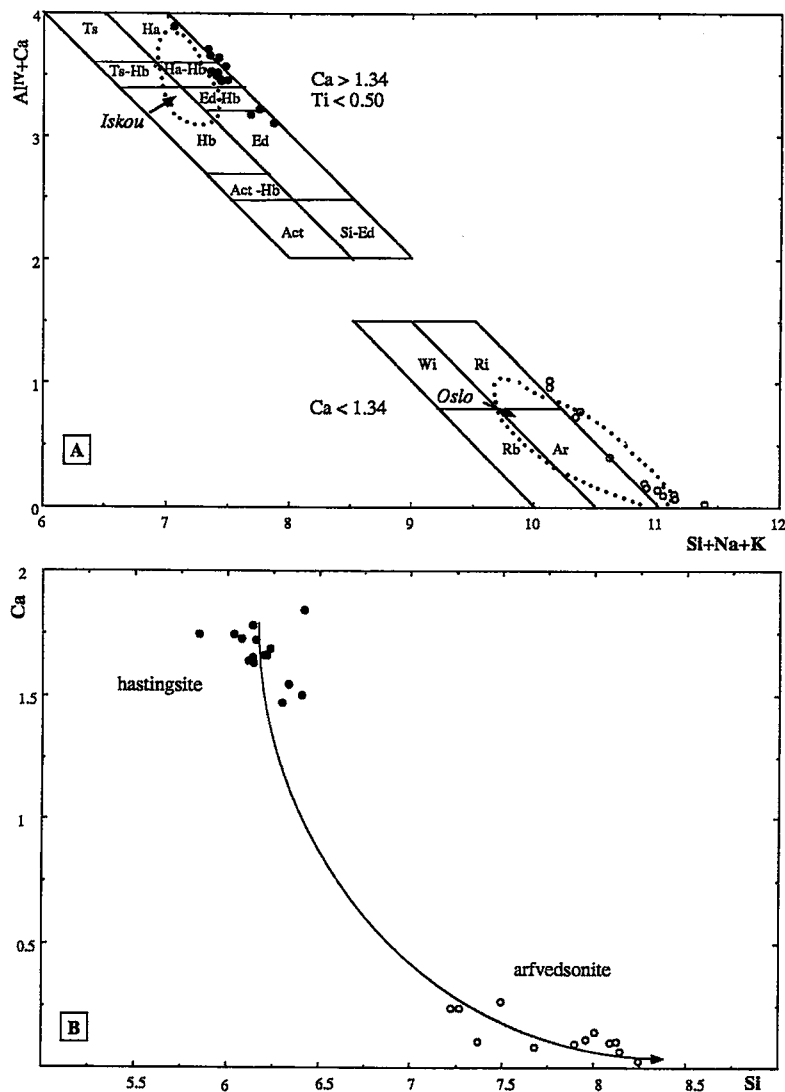


FIG. 4. Composition of the Los amphiboles. A. Amphibole compositions plotted in the  $\text{Ca} + \text{Al}^{\text{IV}} + \text{Ca}$  versus  $\text{Si} + \text{Na} + \text{K}$  diagram (Giret *et al.* 1980). The field of arfvedsonite from the Oslo Rift (Neumann 1976) and the hornblende hastingsite from the Iskou complex (Giret *et al.* 1980) also are shown. B.  $\text{Ca}_B$  versus  $\text{Si}$  diagram (Mitchell 1990). Dots: miaskitic suite; open circles: agpaitic suite.

and Na-Ca pyroxenes, although the manganese content is higher at Los. The niobium content can reach up to 0.52 wt%  $\text{Nb}_2\text{O}_5$  at Los: similar values have been obtained in Zr-rich pyroxene from peralkaline trachyte and comendite from the Warrumbungle volcano (Duggan 1988).

The composition of the amphiboles, also classified according to IMA recommendations (Leake 1978), is calculated on the basis of 13 cations in the tetrahedrally coordinated and C ( $M_1$ ,  $M_2$  and  $M_3$ ) sites. Two groups

have been found: the agpaitic syenite suite is characterized by manganese arfvedsonite, whereas the amphiboles from the miaskitic suite are mostly manganese-magnesian hastingsite or F-rich manganese-magnesian hastingsite (Table 3). In a plot of  $\text{Al}^{\text{IV}} + \text{Ca}$  versus  $\text{Si} + \text{Na} + \text{K}$  (Giret *et al.* 1980) (Fig. 4A), the amphibole compositions from the agpaitic suite evolve from richterite toward arfvedsonite, and plot within the same field as those from the Oslo rift (Neumann 1976). The Los arfvedsonite

TABLE 4. RESULTS OF ELECTRON-MICROPROBE ANALYSES OF REPRESENTATIVE MICA FROM THE LOS ARCHIPELAGO

Sample n°	wt%	Ta35	Ta35	Ta7	Ta7	Ta7	B17
		1	2	3	4	5	6
SiO <sub>2</sub>		37.63	38.27	34.06	35.32	33.9	38.51
TiO <sub>2</sub>		2.29	1.79	1.72	2.72	3.71	2.03
Al <sub>2</sub> O <sub>3</sub>		9.70	9.87	14.93	14.88	15.31	10.55
FeO		19.47	18.77	24.45	22.31	21.66	13.67
MnO		5.63	5.90	4.96	4.52	3.03	5.02
MgO		9.57	10.04	5.48	6.55	7.83	12.93
CaO		0.00	0.00	0.02	0.11	0.06	0.00
Na <sub>2</sub> O		0.31	0.34	0.25	0.32	0.61	0.64
K <sub>2</sub> O		9.74	9.39	9.03	9.11	8.81	9.22
F		1.48	1.46	0.16	0.00	0.14	2.33
Cl		0.15	0.06	0.04	0.01	0.05	0.34
H <sub>2</sub> O calc.		3.75	3.78	3.70	3.80	3.79	3.82
-O=F		0.67	0.66	0.07	0.00	0.06	1.05
-O=Cl		0.07	0.03	0.02	0.00	0.02	0.15
Total		100.46	100.36	98.91	99.65	98.98	100.26
Si		3.006	3.036	2.756	2.784	2.681	3.021
Al iv		0.913	0.923	1.244	1.216	1.319	0.975
Al vi		0.000	0.000	0.180	0.166	0.108	0.000
Ti		0.138	0.107	0.105	0.161	0.221	0.120
Fe <sup>2+</sup>		1.301	1.245	1.654	1.471	1.433	0.897
Mn		0.381	0.396	0.340	0.302	0.203	0.334
Mg		1.140	1.187	0.661	0.770	0.923	1.512
Oct		2.960	2.935	2.940	2.870	2.888	2.863
Ca		0.000	0.000	0.002	0.009	0.005	0.000
Na		0.048	0.052	0.039	0.049	0.094	0.097
K		0.993	0.950	0.934	0.916	0.889	0.923
F		0.374	0.366	0.041	0.000	0.035	0.578
Cl		0.020	0.008	0.005	0.001	0.007	0.045
OH		1.606	1.626	1.954	1.999	1.958	1.377
Total		9.920	9.896	9.915	9.844	9.876	9.879
Fe <sup>2+</sup> /(Fe <sup>2+</sup> + Mg)		0.47	0.49	0.29	0.34	0.39	0.63

(Table 3) is richer in Mn (up to 9.17 wt% MnO) than the arfvedsonite from Kangerdlugssuaq (Kempe & Deer 1970, Layne *et al.* 1982). The amphibole compositions from the miaskitic rocks evolve from hastingsite to hastingsitic hornblende and edenite. The magnesian hastingsite contains up to 3.86 wt% MgO. It is also characterized by a high fluorine content (up to 2 wt%). In the  $\text{Ca}_p$  versus Si diagram (Fig. 4B), the amphibole compositions evolve from magnesian hastingsite toward arfvedsonite, as in other undersaturated complexes (Mitchell 1990).

The compositions of biotite, calculated on the basis of 11 atoms of oxygen, are given in Table 4. The biotite from the rock transitional toward the agpaitic suite (B17 and Ta35) shows a lower Al content (<10 wt% Al<sub>2</sub>O<sub>3</sub>) and iron content, and higher Mn content (up to 5.9 wt% MnO) than the biotite from the miaskitic suite (3–4 wt% MnO). The composition of the low-Al–high-Mn biotite from the agpaitic syenite at Los is very similar to that described at Kangerdlugssuaq (Layne

*et al.* 1982).

The astrophyllite-group minerals occur only in the agpaitic suite. Their composition (calculated on the basis of Si + Al = 8 cations) evolves from astrophyllite (Fe end-member) to kuptekite (Mn end-member) (Table 5). In a single crystal, Mn enrichment can be documented from core to rim (anal. 1 and 2). Compared to astrophyllite from Kangerdlugssuaq (Layne *et al.* 1982), that at Los is richer in Nb (up to 2.34 wt% Nb<sub>2</sub>O<sub>5</sub>).

The lavenite (calculated on the basis of Si + Al = 2 cations) also is a characteristic mineral of the agpaitic suite. At Los, the lavenite (Table 6) is enriched in Ti and Mn compared to that at Kangerdlugssuaq (Kempe & Deer 1970). As at Lovozero (Vlasov *et al.* 1966), it evolves toward titanium-rich lavenite.

In the miaskitic suite, the dominant oxide phase is titaniferous magnetite (calculated on the basis of 3 cations and 4 atoms of oxygen) locally enriched in ulvöspinel component (Table 7). In contrast, in the agpaitic suite, the dominant oxide belongs to the ilmenite group, invariably enriched in Mn, with up to 74 mol.% pyrophanite (Table 8).

The zirconosilicates also are restricted to the agpaitic suite. Representative compositions of catapleite and partial analyses of eudialyte (without REE determinations) are given in Table 9. A mineral close to catapleite, or more probably to  $\alpha$ -hydrocatapleite, NaH<sub>2</sub>ZrSi<sub>3</sub>O<sub>9</sub>·2H<sub>2</sub>O·aq (Portnov *et al.* 1972), calculated on the basis of 3 (Si + Ti + Al) atoms, overgrows the lavenite and the eudialyte. Eudialyte (calculated on the basis of 6 Si atoms) is enriched in Mn (up to 9 wt% MnO), as has been noted by Kunitz (1936) in eudialyte associated with villiaumite and astrophyllite from Roume Island, compared to eudialyte from Lovozero (Khomyakov 1995).

The feldspathoids occur in both suites; representatives compositions are given in Table 10. The sodalite (calculated on the basis of Si + Al + Fe<sup>3+</sup> = 12 cations) is nearly pure. As in the case of sodalite, analcime (calculated on the basis of 96 atoms of oxygen) also is nearly pure. On the contrary, nepheline (calculated on the basis of 32 atoms of oxygen) shows a wide range of K content, from 5.80 to 7.64 wt% K<sub>2</sub>O. In some samples, the nepheline is transformed into cancrinite.

In conclusion, the evolution from miaskitic toward agpaitic suites is marked by drastic changes in the mineral associations and by a general increase in levels of Mn, Zr, and Ti in both the silicates and the oxides that crystallize from the residual liquid. Detailed mineralogical data and discussion of crystallographic substitution within the different minerals will be deferred to a later paper.

#### GEOCHEMISTRY AND AGE OF EMPLACEMENT

Concentrations of major and some trace elements (Zr, Nb, Y, Rb, Sr) in representative samples of

TABLE 5. RESULTS OF ELECTRON-MICROPROBE ANALYSES  
OF REPRESENTATIVE ASTROPHYLLITE AND KUPLETSKITE FROM THE LOS ARCHIPELAGO

sample	Ka27b 1c	Ka27b 1b	K27b 2	Ro9 3	Ro9 4	Ro1 5	Ro1 6	Ro1 7	Ro1 8	Ka1d 9
SiO <sub>2</sub>	32.96	32.55	34.69	32.78	32.82	37.62	34.30	34.54	33.99	33.40
TiO <sub>2</sub>	9.12	9.60	9.11	7.92	8.51	10.83	8.98	10.76	9.20	8.23
ZrO <sub>2</sub>	4.12	2.28	3.06	4.37	3.35	0.52	1.16	0.01	2.90	4.03
Al <sub>2</sub> O <sub>3</sub>	1.26	1.57	1.14	1.62	1.52	0.00	2.06	2.20	1.36	1.70
FeO	22.26	16.22	14.33	18.07	17.51	32.56	17.43	20.98	20.61	15.31
MnO	13.83	18.99	21.92	17.93	18.58	4.64	18.91	15.63	16.18	19.88
MgO	0.62	0.60	0.82	0.32	0.40	0.20	0.94	1.41	0.69	0.68
CaO	1.23	1.62	1.41	1.48	1.56	0.99	1.03	1.77	1.35	1.33
Na <sub>2</sub> O	2.11	1.81	2.02	1.71	1.68	2.66	2.29	1.68	2.11	2.03
K <sub>2</sub> O	5.95	6.12	5.89	6.14	6.01	5.56	5.80	6.22	6.03	5.77
BaO	0.24	0.12	0.22	0.08	n.d.	n.d.	0.14	0.03	0.07	0.07
Nb <sub>2</sub> O <sub>5</sub>	1.71	1.38	n.d.	2.34	2.09	0.70	1.53	n.d.	1.59	
F	0.44	0.49	0.96	0.88	0.82	0.00	0.76	0.92	0.65	0.92
H <sub>2</sub> O calc.	4.55	4.58	4.49	4.44	4.45	4.93	4.86	4.86	4.62	4.54
-O=F	-0.20	-0.22	-0.43	-0.40	-0.37	0.00	-0.34	-0.41	-0.30	-0.41
Total	100.19	97.70	99.62	99.68	98.92	101.21	99.84	100.57	99.47	99.06
Si	6.900	7.095	7.359	7.071	7.123	8.000	6.900	6.843	7.234	7.051
Al	1.100	0.905	0.641	0.929	0.877	0.000	0.000	1.157	0.766	0.949
Z	8.000	8.000	8.000	8.000	8.000	8.000	8.000	8.000	8.000	8.000
Ti	1.359	1.574	1.454	1.285	1.388	1.732	1.359	1.603	1.473	1.309
Zr	0.114	0.242	0.317	0.460	0.355	0.054	0.114	0.001	0.301	0.415
Nb	0.139	0.136	-	0.229	0.205	0.067	0.139	-	-	0.151
Y	1.611	1.953	1.770	1.973	1.949	1.833	1.611	1.604	1.773	1.875
Fe <sup>2+</sup>	2.933	2.956	2.543	3.259	3.179	5.790	2.933	3.476	3.667	2.704
Mn	3.222	3.305	3.938	3.276	3.415	0.836	3.222	2.623	2.917	3.555
Mg	0.281	0.193	0.258	0.102	0.130	0.063	0.281	0.415	0.218	0.213
X	6.436	6.655	6.759	6.638	6.724	6.690	6.436	6.515	6.802	6.472
Ca	0.202	0.380	0.320	0.340	0.360	0.230	0.000	0.380	0.310	0.300
Na	0.894	0.766	0.829	0.713	0.708	1.097	0.894	0.643	0.872	0.832
K	1.488	1.702	1.593	1.691	1.663	1.508	1.488	1.571	1.637	1.553
Ba	0.011	0.010	0.019	0.007	-	-	0.011	0.003	0.006	0.006
W	2.601	2.860	2.760	2.750	2.730	2.840	0.000	2.600	2.820	2.690
F	0.483	0.337	0.645	0.601	0.559	0.000	0.483	0.575	0.440	0.611
OH	6.517	6.663	6.355	6.399	6.441	7.000	6.517	6.425	6.560	6.389
Total W+X+Y+Z	18.660	19.470	19.270	19.360	19.400	19.380	18.660	18.720	19.390	19.040

Columns 1, 5, 7, 8: astrophyllite; columns 2, 3, 4, 6, 9: kupletskeite. Compositions expressed in wt%.

agpaitic and miaskitic syenites and in some dykes and enclaves are given in Table 11, together with their CIPW norms. All the analyzed samples are strongly silica-undersaturated, with normative nepheline content as high as 31% for some agpaitic rocks. In agreement with their modal mineralogy (presence of sodic pyroxene and sodic amphibole), the agpaitic rocks contain up to 7.9% aegirine and sodium metasilicate (*ns*) in their norms, whereas the miaskitic rocks have higher levels of normative magnetite and ilmenite.

The two series of syenite display a restricted range of composition, with SiO<sub>2</sub> between 54 and 60 wt%, and K<sub>2</sub>O + Na<sub>2</sub>O in excess of 13 wt%. They typically plot in the alkaline field of the alkali-silica diagram (Fig. 5). The samples of agpaitic syenite have significantly higher levels of Na and Mn, lower Ti and Ca, higher Na/K, and lower Fe<sup>2+</sup>/Fe<sup>3+</sup> than the samples of miaskitic syenite. The agpaiticity index [the molar ratio (Na + K)/Al], defined by Sørensen (1960), is greater than 1 for the agpaitic rocks and less than 1 for the miaskitic rocks.

Rb, Zr, Nb and Y contents are high for the both types of syenite, as in alkaline rocks in general (Bowden & Turner 1974). The samples of agpaitic

syenite usually show higher concentrations of these elements (with more than 2000 ppm Zr) than those of miaskitic syenite. Agpaitic samples are also characterized by high levels of Rb (usually >300 ppm) and low contents of Sr (<30 ppm), resulting in much higher Rb/Sr values (>20) than in the miaskitic rocks (Rb/Sr < 10).

Samples of phonolite from the ring dykes have major- and trace-element contents roughly similar to those of agpaitic syenite. The two analyzed samples taken from the radial dykes (monchiquite and shonkinite) and the two enclaves (basanite and micro-essexite) have an alkali-rich mafic composition (SiO<sub>2</sub> < 45%).

Rather imprecise K-Ar ages on whole rocks led Lazarenkov (1975) and Lazarenkov & Sherif (1975) to suggest that the Los pluton was emplaced in three phases during the Cretaceous, between 105 to 80 Ma. Ten representative samples of the two syenite series have been analyzed for Rb-Sr isotopes, together with four samples of dykes (two of phonolite from early ring-dykes and two of mafic alkaline character from late radial dykes), a micro-essexite from a large screen and a basanite xenolith. Analytical data are reported in Table 12 and plotted on Figure 6.

TABLE 6. RESULTS OF ELECTRON-MICROPROBE ANALYSES OF REPRESENTATIVE LÄVENITE FROM THE LOS ARCHIPELAGO

sample	Ro9	Ro1	Ro1	Ro1	Ka27b
	1	2	3	4	5
SiO <sub>2</sub>	29.13	29.91	29.67	29.71	29.56
TiO <sub>2</sub>	5.17	6.83	7.31	6.92	8.37
ZrO <sub>2</sub>	20.74	18.51	19.47	18.44	16.66
Nb <sub>2</sub> O <sub>5</sub>	4.82	4.67	3.83	4.47	4.95
Ta <sub>2</sub> O <sub>5</sub>	0.00	0.00	0.27	0.69	0.94
Al <sub>2</sub> O <sub>3</sub>	0.00	0.01	0.03	0.00	0.04
FeO	5.58	4.45	4.18	4.40	4.77
MnO	10.47	10.91	11.51	10.83	10.76
MgO	0.05	0.11	0.14	0.11	0.11
CaO	8.05	9.93	10.33	10.80	9.77
Na <sub>2</sub> O	10.49	10.14	9.95	9.83	10.05
K <sub>2</sub> O	0.02	0.00	0.01	0.00	0.00
BaO	0.03	0.44	0.14	0.18	0.00
F	4.28	3.68	3.70	3.79	3.51
Cl	0.00	0.00	0.05	0.06	0.01
H <sub>2</sub> O calc.	0.16	0.50	0.48	0.43	0.56
-O=F	-1.80	-1.55	-1.56	-1.60	-1.48
-O=Cl	0.00	0.00	-0.01	-0.01	0.00
Total	97.19	98.54	99.50	99.05	98.58
Si	2.000	1.999	1.996	2.000	1.992
Al	0.000	0.001	0.004	0.000	0.008
Ti	0.267	0.343	0.370	0.350	0.424
Zr	0.695	0.603	0.638	0.605	0.548
Nb	0.150	0.141	0.116	0.136	0.151
Fe <sup>2+</sup>	0.321	0.249	0.235	0.247	0.269
Mn	0.609	0.617	0.656	0.617	0.614
Mg	0.005	0.011	0.014	0.011	0.011
Ca	0.592	0.703	0.734	0.771	0.697
Na	1.396	1.314	1.297	1.283	1.313
K	0.002	0.000	0.001	0.000	0.000
Ba	0.001	0.012	0.004	0.005	0.000
F	0.929	0.779	0.786	0.807	0.749
Cl	0.000	0.000	0.000	0.000	0.000
OH	0.071	0.221	0.214	0.193	0.251
Total	6.036	5.994	6.065	6.026	6.026

Concentration of major elements (reported as oxides), fluorine and chlorine reported in wt%.

The computed regression-line calculated for the 16 samples gives a very high MSWD (mean square of the weighted deviates) value of 22.9, which means either that all the samples are not strictly cogenetic (*i.e.*, they have different initial Sr isotopic composition) or that they are not of the same age. Secondary alteration of the isotope system can be ruled out, as petrographically fresh samples only have been measured. If one considers the samples of syenite only (which constitutes the main rock-type of the Los complex), it seems that sample Ka 27b (agpaitic syenite), which has an extremely high <sup>87</sup>Rb/<sup>86</sup>Sr value (528) owing to its very low Sr content (2.66 ppm, isotope dilution), plots distinctly below the regression line. This behavior has been observed before for alkaline rocks with low Sr content, for example in the Noqui peralkaline granite in Zaire (Cahen *et al.* 1976)

TABLE 7. RESULTS OF ELECTRON-MICROPROBE ANALYSES OF REPRESENTATIVE TITANIFEROUS MAGNETITE FROM THE LOS ARCHIPELAGO

sample	Ta18d n°	Bi7 1	Ta7 2	Ta7 3	Ta16 4	Ta16 5	Ta16 6	Ta16 7
SiO <sub>2</sub>	0.05	0.11	0.12	0.08	0.14	0.19	0.04	
TiO <sub>2</sub>	16.33	8.53	6.78	4.42	7.71	7.82	6.70	
Al <sub>2</sub> O <sub>3</sub>	4.80	0.29	0.49	0.51	0.28	0.23	0.68	
Fe <sub>2</sub> O <sub>3</sub> calc.	30.69	50.46	55.19	60.64	54.53	53.86	55.58	
FeO calc.	43.59	26.90	30.81	30.93	31.96	31.79	31.90	
MnO	1.10	11.36	6.69	4.76	6.85	7.02	5.46	
MgO	1.10	0.06	0.03	0.00	0.02	0.00	0.11	
Total	97.67	97.71	100.11	101.34	101.48	100.90	100.47	
Si	0.002	0.004	0.004	0.003	0.005	0.007	0.002	
Ti	0.460	0.250	0.194	0.125	0.218	0.222	0.191	
Al	0.212	0.013	0.022	0.022	0.012	0.010	0.030	
Fe <sup>3+</sup>	0.865	1.478	1.581	1.721	1.542	1.531	1.585	
Fe <sup>2+</sup>	1.363	0.876	0.981	0.976	1.004	1.005	1.011	
Mn	0.035	0.375	0.216	0.152	0.218	0.225	0.175	
Mg	0.061	0.003	0.002	0.000	0.001	0.000	0.006	
End members								
Uvöspinel	0.460	0.250	0.194	0.125	0.218	0.222	0.191	
Fe <sub>2</sub> SiO <sub>4</sub>	0.002	0.004	0.004	0.003	0.005	0.007	0.002	
MnFe <sub>2</sub> O <sub>4</sub>	0.000	0.375	0.216	0.152	0.218	0.225	0.175	
Spinel	0.061	0.003	0.002	0.000	0.001	0.000	0.006	
Hercynite	0.009	0.003	0.009	0.011	0.005	0.005	0.009	
Magnetite	0.432	0.364	0.575	0.709	0.555	0.541	0.617	

Compositions expressed in wt%.

TABLE 8. RESULTS OF ELECTRON-MICROPROBE ANALYSES OF REPRESENTATIVE PYROPHANITE FROM THE LOS ARCHIPELAGO

Sample n°	Ka1d 1	Ka1d 2	Ka1d 3	Ro1 4
SiO <sub>2</sub>	0.04	0.03	0.09	0.21
TiO <sub>2</sub>	51.67	51.00	50.91	49.27
ZrO <sub>2</sub>	0.12	0.07	0.03	0.00
Al <sub>2</sub> O <sub>3</sub>	0.17	0.00	0.00	0.00
Fe <sub>2</sub> O <sub>3</sub> calc.	2.60	2.12	2.68	6.80
FeO calc.	10.39	14.08	13.54	13.08
MnO	35.73	31.44	31.94	31.06
MgO	0.01	0.00	0.01	0.01
CaO	0.03	0.00	0.01	0.00
Total	100.74	98.73	99.20	100.42
Si	0.001	0.001	0.002	0.005
Ti	0.971	0.978	0.972	0.931
Zr	0.001	0.001	0.000	0.000
Al	0.005	0.000	0.000	0.000
Fe <sup>3+</sup>	0.049	0.041	0.051	0.128
Fe <sup>2+</sup>	0.217	0.300	0.287	0.275
Mn	0.756	0.679	0.687	0.661
Mg	0.000	0.000	0.000	0.000
Ca	0.000	0.000	0.000	0.000
Total	2.000	2.000	2.000	2.000
End members				
Gekielite	0	0	0	0
Pyrophanite	74	67	67	62
Ilimenite	21	29	28	26
Hematite	5	4	5	12

Concentration of major elements (reported as oxides), reported in wt%.

TABLE 9. RESULTS OF ELECTRON-MICROPROBE ANALYSES OF  
REPRESENTATIVE CATALPELITE (" $\alpha$ -HYDROCATALELITE")  
AND EUDIALYTE FROM THE LOS ARCHIPELAGO

sample	Ka27b	Kald	Ka27b	Ka27b	sample	Ka27b	Kald	Ka27b	Ka27b
	1	2	3	4		1	2	3	4
SiO <sub>2</sub>	47.96	44.66	51.17	52.45	Si	2.993	2.979	6.000	6.000
TiO <sub>2</sub>	0.00	0.00	0.97	0.45	Al	0.007	0.021	0.096	0.060
ZrO <sub>2</sub>	34.63	33.41	14.29	11.78	Tl	0.000	0.000	0.086	0.039
Nb <sub>2</sub> O <sub>5</sub>	0.00	0.00	0.21	1.72	Zr	1.054	1.087	0.817	0.657
Ta <sub>2</sub> O <sub>5</sub>	0.00	0.44	0.00	0.17	Nb	0.000	0.000	0.011	0.089
Al <sub>2</sub> O <sub>3</sub>	0.04	0.12	0.31	0.20	Ta	0.000	0.000		
FeO	0.00	0.00	3.08	2.64	Fe <sub>2+</sub>	0.000	0.000	0.302	0.253
MnO	0.28	0.00	9.36	8.15	Mn	0.015	0.000	0.930	0.789
MgO	0.00	0.00	0.03	0.05	Mg	0.000	0.000	0.005	0.009
CaO	0.28	0.29	6.34	5.68	Ca	0.019	0.021	0.800	0.700
Na <sub>2</sub> O	8.08	8.09	7.92	12.33	Na	0.978	1.046	1.801	2.736
K <sub>2</sub> O	0.02	0.04	0.17	0.28	K	0.002	0.003	0.025	0.041
BaO			0.00	0.00	Ba			0.000	0.000
F	0.00	0.00	0.28	0.12	F	0.000	0.000	0.104	0.042
Cl	0.00	0.00	0.84	0.71	Cl	0.000	0.000	0.167	0.138
H <sub>2</sub> O calc.	7.50	8.02	0.93	1.07	H <sub>2</sub> O	2.000	2.000	0.729	0.820
-O=F	0.00	0.00	0.12	0.05					
-O=Cl	0.00	0.00	0.19	0.16	Total	7.067	7.157	10.870	11.370
Total	98.79	95.07	95.59	97.60	Concentration of major elements (reported as oxides) fluorine and chlorine reported in wt%. Columns 1 and 2: Cataplelite; column 3 and 4: Endialyte.				

TABLE 10. RESULTS OF ELECTRON-MICROPROBE ANALYSES  
OF REPRESENTATIVE SODALITE, NEPHELINE, AND ANALCIME  
FROM THE LOS ARCHIPELAGO

Sample	Ro1	Ka27b	Ro9	Ta16	Ka27b	Ro9	Ro1	Ta35	Ta16	Ka3	Ta7	Coba	Coba	K27b	Ka3	Ro9
n <sup>b</sup>	1	2	3	4	5	6	7	8	9	10	11	12	13	14	15	16
SiO <sub>2</sub>	37.52	38.88	37.3	37.30	42.03	44.88	41.51	45.14	44.96	45.08	44.20	44.05	43.97	50.67	53.36	54.89
TiO <sub>2</sub>	0.03	0.00	0.00	0.01	0.00	0.03	0.00	0.00	0.00	0.00	0.00	0.03	0.00	0.00	0.03	0.02
Al <sub>2</sub> O <sub>3</sub>	32.53	33.12	31.31	31.70	34.51	32.43	33.605	32.88	32.79	32.58	33.28	32.9	32.76	25.86	30.04	24.16
Fe <sub>2</sub> O <sub>3</sub>	0.43	0.36	0.28	0.15	0.00	0.00	0.00	0.00	0.00	0.00	0.00	0.00	0.00	0.01	0.00	0.34
MnO	0.00	0.00	0.04	0.00	0.00	0.00	0.00	0.045	0.00	0.03	0.01	0.01	0.06	0.03	0.00	0.14
MgO	0.00	0.02	0.04	0.01	0.00	0.00	0.00	0.01	0.00	0.00	0.00	0.00	0.00	0.00	0.00	0.05
CaO	0.01	0.00	0.03	0.04	0.00	0.00	0.00	0.00	0.00	0.33	0.30	0.16	0.12	0.085	0.03	0.01
BaO					0.10	0.00	0.30	0.06	0.00	0.00	0.02	0.14	0.04			
Na <sub>2</sub> O	24.75	24.09	24.73	25.01	15.94	16.20	15.90	16.31	15.92	15.62	15.89	16.29	15.97	15.57	9.47	12.00
K <sub>2</sub> O	0.05	0.00	0.02	0.00	7.58	5.77	7.64	5.62	5.37	5.37	5.68	5.52	5.80	0.11	0.03	0.13
SO <sub>3</sub>	0.38	0.47	0.00	0.00												
F	0.00	0.00	0.00	0.00												
Cl	7.20	6.74	8.12	8.00												
-O=Cl	-1.62	-1.52	-1.83	-1.80												
-O=S	-0.05	-0.05	0.00	0.00												
H <sub>2</sub> O calc.														8.47	8.50	8.27
Total	100.83	101.63	100.04	100.41	100.16	99.31	99.00	100.03	99.4	98.96	99.24	99.11	98.65	100.72	101.58	99.94
Si	5.910	5.968	6.015	5.986	8.115	8.555	8.176	8.573	8.555	8.625	8.444	8.472	8.473	29.978	30.272	31.979
Tl	0.004	0.000	0.000	0.002	0.000	0.004	0.000	0.000	0.000	0.000	0.000	0.005	0.000	0.000	0.014	0.01
Al	6.039	5.991	5.951	5.996	7.853	7.285	7.801	7.359	7.354	7.347	7.493	7.459	7.439	18.031	20.089	16.59
Fe <sub>3+</sub>	0.051	0.041	0.034	0.018	0.032	0.160	0.023	0.068	0.091	0.028	0.062	0.069	0.088	0.005	0.000	0.151
Mn	0.000	0.000	0.005	0.000	0.000	0.000	0.008	0.000	0.006	0.002	0.002	0.010	0.004	0.000	0.068	0.043
Mg	0.000	0.004	0.008	0.001	0.000	0.000	0.000	0.000	0.000	0.000	0.000	0.000	0.000	0.000	0.002	0.042
Ca	0.001	0.000	0.006	0.006	0.000	0.000	0.000	0.000	0.067	0.061	0.032	0.025	0.018	0.019	0.006	0.000
Ba					0.007	0.000	0.023	0.005	0.000	0.000	0.002	0.010	0.003			
Na	7.559	7.169	7.731	7.782	5.968	5.989	6.072	6.007	5.872	5.793	5.884	6.076	5.965	17.860	10.418	13.557
K	0.009	0.000	0.005	0.000	1.867	1.404	1.921	1.362	1.303	1.311	1.384	1.354	1.427	0.083	0.02	0.097
F	0.000	0.000	0.000	0.000												
Cl	1.922	1.753	2.220	2.175												
S	0.045	0.054	0.000	0.000												
H <sub>2</sub> O														16.713	16.084	16.069
Total	21.540	20.980	21.975	21.966	23.842	23.397	24.024	23.376	23.248	23.167	23.303	23.480	23.417	65.976	60.888	62.468

Columns 1 to 4: sodalite; columns 5 to 13: nepheline; columns 14 to 16: analcime. Compositions expressed in wt%.

TABLE 11. CHEMICAL COMPOSITION OF REPRESENTATIVE SAMPLES FROM THE LOS ARCHIPELAGO

	Ka27b	Ro9	Ro1	Kald	Ta35	Co6a	BL7	Ta16	Ka3	Ta7	Ta9	Ca4	Ro13e	Ta18d	Co3a	Ta5c
SiO <sub>2</sub>	55.59	54.00	55.28	58.28	60.63	54.98	59.36	56.12	56.40	59.45	56.34	56.47	44.78	43.47	44.04	43.62
TiO <sub>2</sub>	0.26	0.23	0.20	0.21	0.57	1.02	0.43	0.52	0.36	0.76	0.32	0.24	1.93	2.53	2.30	2.52
Al <sub>2</sub> O <sub>3</sub>	20.89	21.32	21.37	20.63	18.16	18.93	19.53	21.86	22.05	19.28	20.19	20.63	15.46	14.21	12.17	13.41
Fe <sub>2</sub> O <sub>3</sub>	2.72	1.60	1.93	1.54	2.71	1.28	2.20	0.76	1.01	1.49	1.21	1.23	3.90	4.86	3.54	5.21
FeO	0.70	0.95	0.50	0.87	0.47	2.61	1.55	1.15	1.59	1.16	1.04	1.04	5.21	5.46	7.12	7.53
MnO	0.48	0.46	0.36	0.45	0.30	0.37	0.48	0.21	0.36	0.23	0.31	0.29	0.25	0.18	.21	0.20
MgO	0.13	0.16	0.24	0.17	0.13	0.77	0.21	0.34	0.39	0.34	0.20	0.19	5.09	7.31	8.97	8.98
CaO	0.59	0.98	0.86	0.27	0.59	2.82	0.75	1.18	1.56	1.67	1.08	1.07	7.72	10.46	12.19	12.90
Na <sub>2</sub> O	11.69	10.48	9.87	10.62	7.97	7.74	8.75	8.48	8.49	6.28	9.66	9.54	5.49	3.37	4.17	2.78
K <sub>2</sub> O	4.70	6.07	5.49	4.58	6.14	6.73	4.98	7.07	6.26	7.46	5.81	5.68	3.22	2.14	2.23	1.05
P <sub>2</sub> O <sub>5</sub>	0.01	0.02	0.02	0.01	0.03	0.14	0.03	0.05	0.03	0.07	0.03	0.08	0.69	0.63	0.59	0.49
L.O.L.	1.25	2.97	3.48	1.18	2.00	1.77	1.38	1.97	0.90	1.66	3.46	2.90	5.91	5.22	2.24	1.14
Total	99.01	99.24	99.60	98.81	99.70	99.16	99.65	99.71	99.40	99.85	99.65	99.36	99.65	99.84	99.77	99.83
Zr ppm	2272	1741	1466	2041	742	593	1321	368	1271	345	1243	1135	289	215	213	
Nb ppm	439	449	331	398	255	208	487	164	280	196	270	205	135	106	68	62
Y ppm	37	30	36	26	49	49	43	24	37	34	29	25	33	28	29	29
or	27.77	35.87	32.44	27.07	36.29	39.77	29.43	41.78	36.99	44.09	34.34	33.57	19.03	12.65	13.18	6.21
ab	27.19	17.35	27.50	40.29	41.18	16.88	46.66	22.48	26.98	34.86	28.18	29.23	11.73	11.90	0.00	9.26
an	0.00	0.00	0.00	0.00	0.00	0.00	0.00	0.70	3.57	2.39	0.00	0.00	8.03	17.33	7.90	21.01
ne	29.31	31.70	28.09	21.85	9.78	23.31	14.12	26.70	24.30	9.90	23.47	24.52	18.81	9.00	19.12	7.73
ac	7.87	4.63	3.66	4.45	7.24	3.71	1.16	0.00	0.00	0.00	3.50	3.56	0.00	0.00	0.00	0.00
ms	2.03	1.76	0.00	0.98	0.00	0.32	0.00	0.00	0.00	0.00	1.46	0.51	0.00	0.00	0.00	0.00
di (wo)	1.20	1.98	1.32	0.53	0.64	5.46	1.47	1.87	1.66	1.04	2.15	2.00	10.76	12.71	20.34	16.61
di (en)	0.20	0.33	0.60	0.10	0.32	1.88	0.39	0.85	0.53	0.85	0.47	0.40	7.63	10.08	14.30	12.01
di (fs)	1.09	1.82	0.71	0.48	0.31	3.73	1.16	1.02	1.18	0.07	1.83	1.74	2.18	1.20	4.31	3.08
wo	0.00	0.00	0.41	0.00	0.49	0.08	0.00	0.14	0.00	1.23	0.00	0.00	0.00	0.00	0.00	0.00
ol (fo)	0.09	0.05	0.00	0.23	0.00	0.02	0.09	0.00	0.31	0.00	0.02	0.05	3.54	5.70	5.64	7.26
ol (fa)	0.51	0.31	0.00	1.24	0.00	0.05	0.30	0.00	0.75	0.00	0.10	0.24	1.11	0.75	1.88	2.05
mt	0.00	0.00	0.96	0.00	0.30	0.00	2.61	1.10	1.46	2.16	0.00	0.00	5.65	7.05	5.13	7.56
il	0.49	0.44	0.38	0.40	1.08	1.94	0.82	0.99	0.68	1.44	0.61	0.46	3.67	4.80	4.37	4.79
ap	0.02	0.05	0.05	0.02	0.07	0.32	0.07	0.11	0.07	0.16	0.07	0.18	1.59	1.45	1.36	1.13
(Na+K)/Al	1.16	1.12	1.04	1.09	1.09	1.06	1.01	0.99	0.94	0.95	1.10	1.06	0.81	0.55	0.76	0.43

Concentration of major elements reported as oxides in wt%, and of trace elements reported in ppm.

and the Kidal ring-complex of the Iforas, Mali (Liégeois & Black 1984). Disregarding this sample, the nine samples of syenite plot on a good isochron (MSWD = 1.28), which gives an Albian age, 104.3 ± 1.7 Ma (2σ), with an initial ratio of 0.70401 ± 0.00008 (2σ).

The micro-essexite screen (sample Co 3a) and the basanite enclave (sample Ta 5c), which have virtually the same measured Sr isotopic composition and very low <sup>87</sup>Rb/<sup>86</sup>Sr ratios (0.19 and 0.16, respectively), plot very close to the isochron. The computed line for the 11 samples [104.5 ± 1.6 Ma; (<sup>87</sup>Sr/<sup>86</sup>Sr)<sub>0</sub> = 0.70399 ± 0.00004; MSWD = 1.04] is, within error limits, indistinguishable from the "syenite" isochron. The two analyzed samples of phonolite dykes, which are geochemically similar to the syenites, also plot, within errors limits, on the "syenite" isochron, suggesting a comagmatic origin.

The late radial dykes (monchiquite and micro-

shonkinite) on the contrary, plot slightly but significantly below the isochron: they have initial ratios (calculated at 105 Ma) close to 0.7033. This value is compatible with a mantle-derived mafic magma without crustal influence; the slightly higher isotopic ratio of the syenitic and phonolitic rocks (0.7040) points either to a different mantle source-region or to some degree of crustal contamination during emplacement and differentiation of the Los complex. The lack or low level of crustal contamination in nepheline syenite compared to quartz syenite has been reported in other syenitic complexes, such as Marangudzi, Zimbabwe and Mont Brome, Quebec (Foland *et al.* 1993) and from the Abu Khurq complex, Egypt, in which the contamination is related to the silica saturation of the magma (Landoll *et al.* 1994). The lack of quartz syenite in the Los archipelago is attributed to the emplacement of the archipelago at the edge of a passive margin.

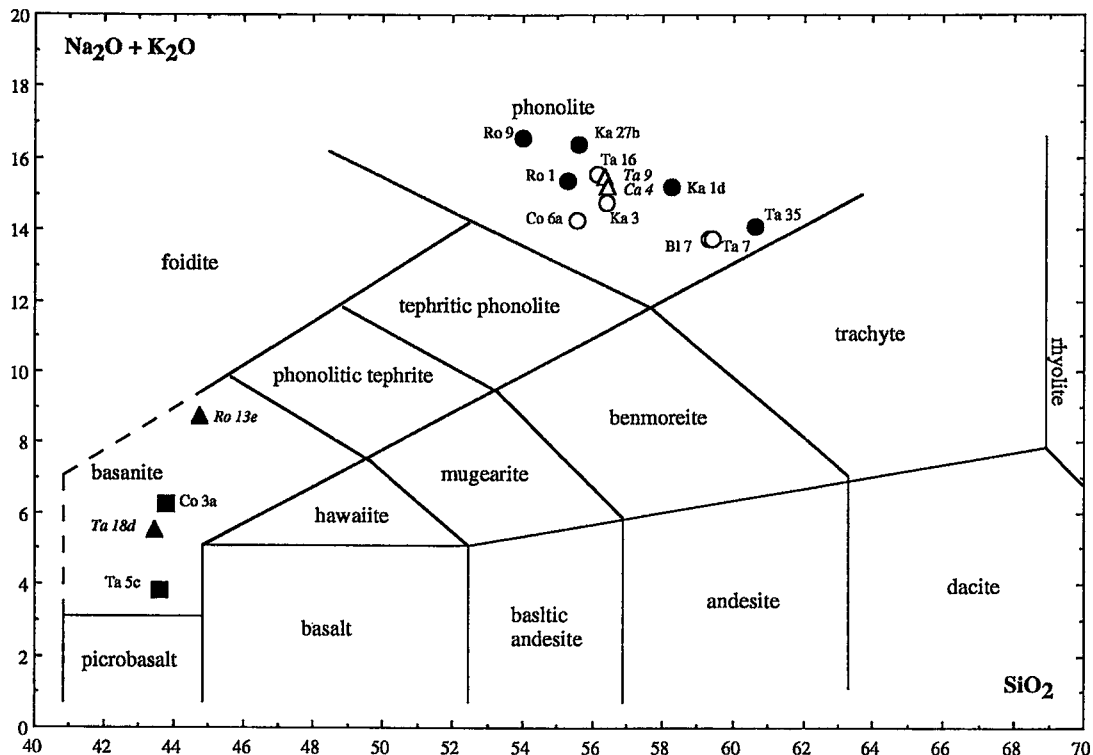


FIG. 5. Total alkali versus silica (TAS) diagram. Volcanic fields after Le Bas *et al.* (1986) and Le Maitre (1989).

TABLE 12. Rb-Sr ISOTOPIC DATA FOR SELECTED SAMPLES FROM THE LOS ARCHIPELAGO

N°	Samples	Rock-type	Rb (ppm)	Sr (ppm)	$^{87}\text{Rb}/^{86}\text{Sr}$	$^{87}\text{Sr}/^{86}\text{Sr}$	2 sigma
1	Ka 27b	agpaitic syenite	445	2.66 *	528	1.63375	0.00040
2	Ro 9	agpaitic syenite	412	7.67 *	159	0.93749	0.00035
3	Ro 1	agpaitic syenite	371	9.10 *	120	0.88729	0.00030
4	Ka 1d	agpaitic syenite	404	17.80 *	66.3	0.80547	0.00027
5	Ta 35	agpaitic syenite	296	9.80 *	88.5	0.83237	0.00007
6	BI 7	miasikitic syenite	254	32.0 *	23.1	0.73748	0.00006
7	Ta 16	miasikitic syenite	192	87	6.44	0.71331	0.00003
8	Ka 3	miasikitic syenite	253	223	3.29	0.70891	0.00004
9	Ta 7	miasikitic syenite	179	246	2.11	0.70715	0.00003
10	Co 6a	miasikitic syenite	198	1335	0.43	0.70466	0.00005
11	Ta 9	phonolite	315	8.30 *	112	0.87417	0.00010
12	Ca 4	phonolite	271	53	14.9	0.72643	0.00007
13	Ro 13e	monchiquite	192	857	0.65	0.70443	0.00002
14	Ta 18d	micro-shonkinite	58	950	0.18	0.70360	0.00004
15	Co 3a	micro-essexite (screen)	78	1177	0.19	0.70427	0.00002
16	Ta 5c	basanite (xenolith)	43	778	0.16	0.70422	0.00003

\* Isotope dilution method

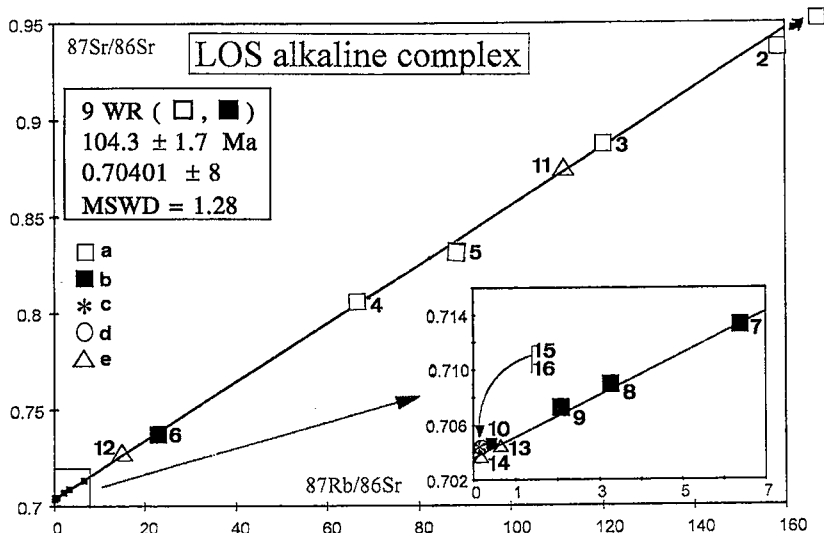


FIG. 6. Rb-Sr whole-rock isochron for the Los suite of syenites. a: agpaitic suite; b: miaskitic suite; c: micro-essesite; d: basanite; e: dykes (phonolite, shonkinite and monchiquite). For more details, see Table 2 and text.

#### DISCUSSION:

#### THE LOS ARCHIPELAGO IN RELATION WITH THE EVOLUTION OF CENTRAL-EQUATORIAL ATLANTIC OCEAN

Post-Paleozoic magmatic activity in West Africa is commonly subdivided into three periods (Sykes 1978, Guiraud *et al.* 1987): 1) a short and widespread Liassic magmatic event, well dated from  $203.7 \pm 2.7$  Ma to  $197.1 \pm 1.8$  Ma (Sebai *et al.* 1991), has affected a 2000-km-long area along the edge of the West African craton. It has produced abundant continental tholeiite occurring as diabase dykes (Dars 1960) and sills (Bertrand 1991). Two laccolithic intrusive bodies are related to this event: the Kakoulima body in Guinea (Lazarenkov 1975, Diallo *et al.* 1992) and the Freetown body in Sierra Leone (Briden *et al.* 1971). 2) Numerous pipes and dykes of kimberlite are scattered over Liberia, Sierra Leone, Guinea and Mali; their early Cretaceous age (140 to 92 Ma; Odin 1994) is based on paleomagnetic evidence (Haggerty 1982). 3) Cenozoic alkaline volcanism occurs along the West African margin (Cape Verde and Canary archipelagos, Dakar Peninsula). A huge volcanic seamount has been discovered on the southern margin of the Guinean continental shelf (Bertrand *et al.* 1988, 1989).

The Guinean continental shelf is bounded to the West by the southernmost segment of the Central Atlantic passive margin of Jurassic age, and to the South by a transform-type margin related to the Equatorial Atlantic opening (Bertrand *et al.* 1989). The

Guinean margin has been subjected to several magmatic events related to tectonic changes in the drift of the southern continents (Africa, South America). The tholeiitic magmatism at  $\sim 200$  Ma has been linked (Bertrand 1991) to extensional tectonism related to a rifting mechanism that eventually led to continent disruption. In early Cretaceous time, the margin became a transform margin with the development of E-W fracture shear-zone (like the actual St. Paul and Romanche faults in the Equatorial Atlantic). This shear or transform zone allowed a connection between rifting in the Northern and in the Southern Atlantic (Mascole *et al.* 1995). This Barremian to Albian (117 to 96 Ma) transtensional tectonic phase resulted in the formation of small pull-apart basins characterized by the thinning of the continental crust (Mascole *et al.* 1986, 1988), and the progressive opening of the Equatorial Atlantic Ocean between West Africa and South America. This phase was accompanied by the emplacement of alkaline igneous rocks along fault zones, like the Liberian and Sierra Leone kimberlites, which intruded along reactivated crustal fractures, as suggested by Haggerty (1982). The southern Guinean margin was formed by the reactivation of one of the Guineo-Nubian lineaments (Guiraud *et al.* 1987), of Jurassic age.

The final disruption between the West African and South American continents resulted in a pronounced tectonic unconformity of upper Albian age ( $\sim 100$  Ma) (Mascole *et al.* 1986, 1988, 1995, Wilson & Guiraud 1992). It resulted in the complete relaxation of shear

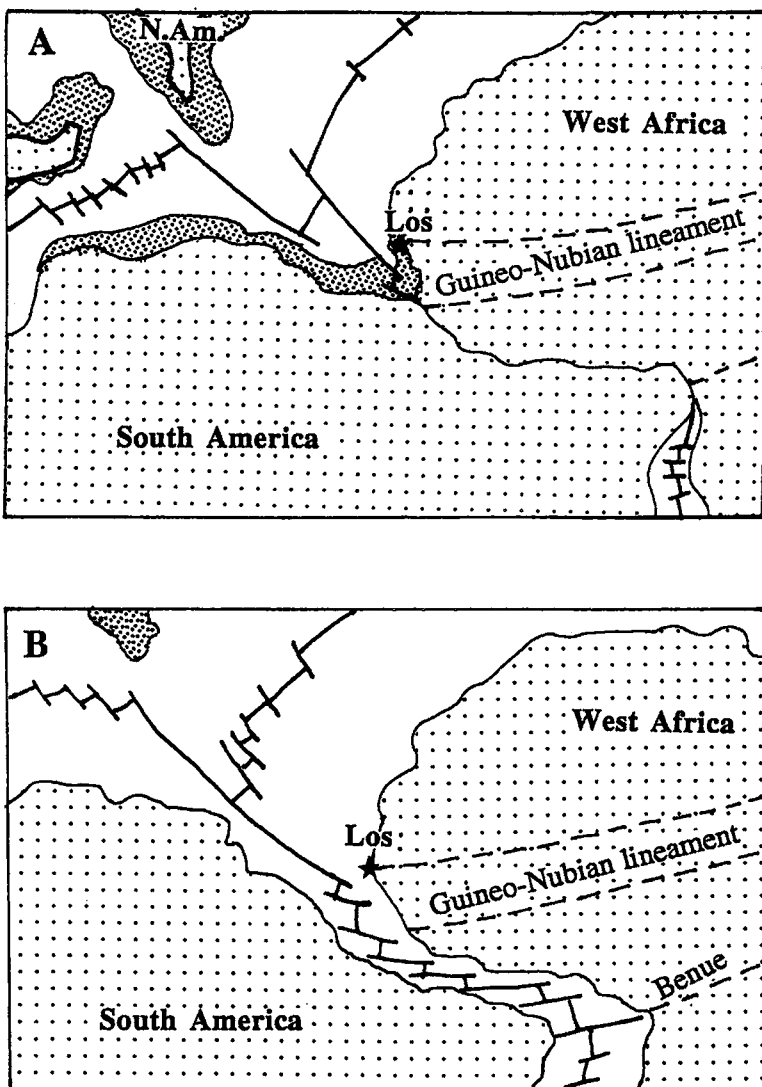


FIG. 7. Paleoenvironmental maps (modified after Dercourt *et al.* 1993). A. Early Aptian (113–108 Ma) plate tectonic reconstruction, with the future position of the Los Archipelago. B. Late Cenomanian (96–92 Ma) plate tectonic reconstruction, with the location of the Los Archipelago after its emplacement.

stresses. During Cenozoic times, minor changes in the pattern of drifting in the central Atlantic have produced local tensional stresses (along old fractures of the West African margin), which are possibly responsible for the alkaline volcanism.

The Los syenite ring-structure, dated at  $104.3 \pm 1.7$  Ma (Albian), thus appears to have been emplaced at the end of this transtensional tectonic phase, during the early opening of the Equatorial Atlantic Ocean. On the paleoenvironmental map for Aptian times (113–108 Ma) (Fig. 7A, from Dercourt *et al.* 1993), the geological setting of the Los area is the Jurassic passive

margin of the central Atlantic. The magmatic pulse thus occurred in an attenuated continental crust by reactivation of a prominent east–west fracture. This happened as a result of relaxation of shear stress, implying a tensional gash oblique to the Guineo-Nubian lineament. The paleoenvironmental map for late Cenomanian (96–92 Ma) times (Fig. 7B, Dercourt *et al.* 1993) shows clearly the opening of the Equatorial Atlantic Ocean and the progressive westward offset of the spreading ridge along prominent transform faults in the prolongation of the Guineo-Nubian lineaments.

## CONCLUSIONS

1. The Los ring-complex intruded the Guinean passive continental margin, which consists of a Proterozoic basement covered by early Mesozoic sediments.
2. The Los complex consists mainly of nepheline syenites cut by phonolite dykes and by alkaline mafic dykes (monchiquite, shonkinite).
3. Two suites of rocks have been recognized, one miaskitic, the other agpaitic.
4. These suites differ by their mafic minerals. Samples of miaskitic syenite contain augite, hastingsitic amphibole, Mn-bearing mica and titanite. Samples of agpaitic syenite are characterized by aegirine, Mn-rich arfvedsonite, Mn-rich mica, pyrophanite, kupletsksite and lavenite, and by Zr- and REE-rich accessory minerals (eudialyte, catapleiite, pyrochlore).
5. All the syenites are enriched in elements (Rb, Zr, Nb, Y) typically found in alkaline rocks, the agpaitic syenite being more strongly enriched (>300 ppm Rb, up to 2000 ppm Zr) than the miaskitic syenite.
6. The phonolite found in dykes is similar geochemically to the agpaitic syenite.
7. An Albian age ( $104.3 \pm 1.7$  Ma; Rb-Sr whole-rock isochron) has been obtained for the emplacement of the Los complex.
8. The low initial  $^{87}\text{Sr}/^{86}\text{Sr}$  value ( $0.70401 \pm 0.00008$ ) points to a mantle origin without significant crustal influence.
9. The intrusion of the Los complex is related to the end of a transtensional tectonic regime during the early opening of the Equatorial Atlantic ocean, along reactivated Guineo-Nubian lineaments.

## ACKNOWLEDGEMENTS

Thanks are extended to Dr. K. Bell (Carleton University, Ottawa) and Dr. L. Kogarko (Vernadsky Institute of Geochemistry, Moscow) for I.G.C.P. (project 314 "Alkaline and carbonatitic magmatism") funding to D.O. to participate at the special symposium on "The petrology, mineralogy and geochemistry of alkaline rocks" at the Waterloo's GAC-MAC meeting in May 1994. C.M. acknowledges with gratitude the C.N.R.S research grant "Action Spéciale Programmée Afrique", coordinator Dr. M. Deynoux. D.D. thanks the FNRS, which gives financial support for isotopic measurements at Bruxelles. Dr. K.A. Foland (Ohio State University, Columbus) and an anonymous referee, as well as R.F. Martin, are thanked for their careful review and improvement of an earlier draft of the manuscript.

## REFERENCES

- BARRÈRE, J. (1959): La presqu'île du Kaloum et le massif de Kakoulima (République de Guinée). *Serv. Géol. Prospl. Minière, Dakar* **2**, 7-44.
- BECKINSALE, R.D., BOWLES, J.F.W., PANKHURST, R.J. & WELLS, M.K. (1977): Rubidium-strontium age studies and geochemistry of acid veins in the Freetown complex, Sierra Leone. *Mineral. Mag.* **41**, 501-511.
- BERTRAND, H. (1991): The Mesozoic tholeiitic province of northwest Africa: a volcanotectonic record of the early opening of central Atlantic. In *Magma in Extensional Structural Settings: the Phanerozoic African Plate* (A.B. Kampunzu & R.T. Lubala, eds.). Springer-Verlag, Berlin, Germany (147-188).
- \_\_\_\_\_, MASCLE, J., MARINHO, M. & VILLENEUVE, M. (1988): Volcanics from the Guinean continental margin: geodynamic implications. *J. Afr. Earth Sci.* **7**, 181-188.
- \_\_\_\_\_, \_\_\_\_\_, VILLENEUVE, M., ROBERT, C., COUSIN, M. ET LE GROUPE EQUAMARGE (1989): Le volcanisme de la marge sud guinéenne, implications pour l'ouverture de l'Atlantique équatorial: résultats de la campagne Equamarge II. *C.R. Acad. Sci. Paris* **309**, Sér. II, 1703-1708.
- BLACK, R., LAMEYRE, J. & BONIN, B. (1985): The structural setting of alkaline complexes. *J. Afr. Earth Sci.* **3**, 5-16.
- BOWDEN, P. & TURNER, D.C. (1974): Peralkaline and associated ring-complexes in the Nigeria-Niger province, West Africa. In *The Alkaline Rocks* (H. Sørensen, ed.). John Wiley & Sons, London, U.K. (330-351).
- BRIDEN, J.C., HENTHORN, D.I. & REX, D.C. (1971): Palaeomagnetic and radiometric evidence for the age of the Freetown igneous complex, Sierra Leone. *Earth Planet. Sci. Lett.* **12**, 385-391.
- CAHEN, L., DELHAL, J. & LEDENT, D. (1976): Chronologie de l'orogenèse ouest-congolienne et comportement isotopique de roches d'alcalinité différente dans la zone interne de l'orogène, au Bas Zaïre. *Ann. Soc. géol. Belg.* **99**, 189-203.
- CANTAGREL, F. & PIN, C. (1994): Major, minor and rare earth element determination in 25 rock standards by ICP atomic emission spectrometry. *Geostandards Newslett.* **18**(1), 123-138.
- CRÉVOLA, G., CANTAGREL, J.M. & MOREAU, C. (1994): Le volcanisme cénozoïque de la presqu'île du Cap Vert (Sénégal): âge, caractères et cadre géodynamique. *Soc. géol. Fr., Bull.* **165**, 5, 437-446.
- DARS, R. (1960): *Les formations sédimentaires et les dolérites du Soudan occidental (Afrique de l'Ouest)*. Thèse de doctorat, Univ. de Paris, Paris, France.
- DELAIRE, L. & RENAUD, L. (1955): Carte géologique de reconnaissance à l'échelle du 1/500 000° et notice explicative: Conakry Ouest. Direct. Mines, A.O.F., Dakar, Sénégal.
- DERCOURT, J., RICOU, L.E. & VRIELYNCK, J.M. (1993): *Atlas Tethys: Palaeoenvironmental Maps*. Gauthier-Villars, Paris, France.

- DIALLO, D., BERTRAND, H., AZAMBRE, B., GRÉGOIRE, M. & CASEIRO, J. (1992): Le complexe basique-ultrabasique du Kakoulima (Guinée-Conakry): une intrusion tholéïtique stratifiée liée au rifting de l'Atlantique central. *C.R. Acad. Sci. Paris*, **314**, Sér. II, 937-943.
- DUDKIN, O.B. & MITROFANOV, F.P. (1994): Features of the Kola alkali province. *Geochem. Int.* **31**(3), 1-11.
- DUGGAN, M.B. (1988): Zirconium-rich sodic pyroxenes in felsic volcanics from the Warrumbungle volcano, central New South Wales, Australia. *Mineral. Mag.* **52**, 491-496.
- FOLAND, K.A., LANDOLL, J.D., HENDERSON, C.M.B. & CHEN, JIANG-FENG (1993): Formation of cogenetic quartz and nephelines syenites. *Geochim. Cosmochim. Acta* **57**, 697-704.
- GIRET, A., BONIN, B. & LÉGER, J.M. (1980): Amphibole compositional trends in oversaturated and undersaturated alkaline plutonic ring-complexes. *Can. Mineral.* **18**, 481-495.
- GUIRAUD, R., BELLION, Y., BENKHEILI, J. & MOREAU, C. (1987): Post-Hercynian tectonics in northern and western Africa. In *African Geology Reviews* (P. Bowden & J. Kinnaird, eds.). John Wiley & Sons, London, U.K. (433-466).
- GÜRICH, G. (1887): Beiträge zur Geologie von Westafrika, Z. *Deutsch. Geol. Gesell.* **39**, 96-135.
- HAGGERTY, S.E. (1982): Kimberlites in western Liberia: an overview of the geological setting in a plate tectonic framework. *J. Geophys. Res.* **87**, 10811-10826.
- HENOC, J. & TONG, M. (1978) Automatisation de la microsonde. *J. Microsc. Spectrosc. Electr.* **3**, 247-254.
- KEMPE, D.R.C. & DEER, W.A. (1970): Geological investigations in east Greenland. IX. The mineralogy of the Kangerdlugssuaq alkaline intrusion, east Greenland. *Medd. om Grønland* **190**, 1-95.
- KHOMYAKOV, A.P. (1995): *Mineralogy of Hyperalpatic Alkaline Rocks*. Clarendon Press, Oxford, U.K.
- KUNITZ, W. (1936): Die Rolle des Titans und Zirconiums in den gesteinbliden-Silikaten. *Neues Jahrb. Mineral. Paläont.* **70A**, 385-466.
- LACROIX, A. (1908): Sur l'existence du fluorure de sodium cristallisé comme élément des syénites néphéliniques des îles de Los. *C.R. Acad. Sci. Paris* **146**, 213-216.
- \_\_\_\_\_(1911): Les syénites néphéliniques de l'archipel de Los et leurs minéraux. *Nouv. Arch. Mus. Hist. Nat.* **3**, 1-132.
- \_\_\_\_\_(1931): Les pegmatites de la syénite sodalitique de l'île Rouma (archipel de Los, Guinée française). Description d'un nouveau minéral (sérandite) qu'elles renferment. *C.R. Acad. Sci. Paris* **192**, 189-194.
- LANDOLL, J.D., FOLAND, K.A. & HENDERSON, C.B.M. (1994): Nd isotopes demonstrate the role of contamination in the formation of coexisting quartz and nepheline syenites at the Abu Khurq Complex, Egypt. *Contrib. Mineral. Petrol.* **117**, 305-329.
- LARSEN, L.M. (1976): Clinopyroxenes and coexisting mafic minerals from the alkaline Ilfmaussaq intrusion, south Greenland. *J. Petrol.* **17**, 258-290.
- \_\_\_\_\_- & SØRENSEN, H. (1987): The Ilfmaussaq intrusion – progressive crystallization and formation of layering in an agpaitic magma. In *Alkaline Igneous Rocks* (J.G. Fitton & B.G.J. Upton, eds.). *Geol. Soc., Spec. Pap.* **30**, 473-488.
- LAYNE, G.D., RUCKLIDGE, J.C. & BROOKS, C.T. (1982): Astrophyllite from Kangerdlugssuaq, East Greenland. *Mineral. Mag.* **45**, 149-156.
- LAZARENKO, V.G. (1975): *Les syénites feldspathoïdiques des îles de Los (Guinée)*. Thèse de Doctorat, Univ. de Moscou, Moscou, Russie (en Russe).
- \_\_\_\_\_- & SHERIF, M. (1975): Chemical composition of the Los pluton, Republic of Guinea. *Dokl. Acad. Sci. USSR, Earth Sci. Sect.* **224**(4), 199-201.
- LEAKE, B.E. (1978): Nomenclature of amphiboles. *Am. Mineral.* **63**, 1023-1052.
- LE BAS, M.J., LE MAITRE, R.W., STRECKEISEN, A. & ZANETTI, B. (1986): A chemical classification of volcanic rocks based on the total alkali – silica diagram. *J. Petrol.* **27**, 745-750.
- LE MAITRE, R.W. (1989): *A Classification of Igneous Rocks and Glossary of Terms*. Blackwell Scientific Publ., London, U.K.
- LIFÉGOIS, J.P. & BLACK, R. (1984): Pétrographie et géochronologie Rb–Sr de la transition calco-alcaline fini-panafricaine dans l'Adrar des Iforas (Mali): accrétion crustale au Précambrien supérieur. In *Géologie africaine* (J. Klerkx et J. Michot, eds.). *Musée Roy. Afr. Centr. (Tervuren)*, 115-145.
- MASCLE, J., BIAREZ, E. & MARINHO, M. (1988): The shallow structures of the Guinea and Ivory Coast – Ghana transform margins: their bearing on the equatorial Atlantic Mesozoic evolution. *Tectonophys.* **155**, 193-209.
- \_\_\_\_\_, LOHMANN, G.P. & CLIFT, P. (1995): La marge transformante de Côte-d'Ivoire – Ghana: premiers résultats de la campagne ODP 159 (janvier-février 1995). *C.R. Acad. Sci. Paris* **320**, 737-747.
- \_\_\_\_\_, MARINHO, M. & WANNESSEN, J. (1986): The structure of the Guinean continental margin: implications for the connection between the central and the south Atlantic Oceans. *Geol. Rundsch.* **75**, 57-70.

- MILLOT, G. & DARS, R. (1959): L'archipel des îles de Los: une structure annulaire subvolcanique (République de Guinée). *Serv. Géol. Prospe. Minière, Dakar* 2, 50-56.
- MITCHELL, R.H. (1990): A review of the compositional variation of amphiboles in alkaline plutonic complexes. *Lithos* 26, 135-156.
- MOREAU, C., ROBINEAU, B., BAH, M.S. & CAMARA, I.S. (1986): Caractères pétrographiques et géométriques d'une structure annulaire de syénites néphéliniques: l'archipel des îles de Los (Guinée). *C.R. Acad. Sci. Paris* 303, Sér. II, 71-74.
- MORIMOTO, N. (1988): Nomenclature of pyroxenes. *Mineral. Mag.* 52, 535-550.
- NEUMANN, E.R. (1976): Compositional relations among pyroxenes, amphiboles and other mafic phases in the Oslo region plutonic rocks. *Lithos* 9, 85-109.
- ODIN, G.S. (1994): Geological time scale (1994). *C.R. Acad. Sci. Paris*, 318, Sér. II, 59-71.
- PARODI, G.C. & DELLA VENTURA, G. (1987): Steacyite from the Rouma Isle (Los Islands, Republic of Guinea). *Neues Jahrb. Mineral., Monatsh.*, 233-239.
- PONTNOV, A.M., DUBINCHUK, V.T. & SOINTSEVA, L.S. (1972): Nonsymmetric isomorphism and three-dimensional polytypy in minerals of the catapleiite group. *Dokl. Acad. Sci. USSR, Earth Sci. Sect.* 202, 122-125.
- POUCHOU, J.L. & PICHOIR, F. (1984): Un nouveau modèle de calcul pour la microanalyse quantitative par spectrométrie de rayons X. *Recherche Aérospat.* 3, 167-192.
- \_\_\_\_\_, & \_\_\_\_\_. (1991): Quantitative analysis of homogeneous or stratified microvolumes applying the model "PAP". In *Electron Probe Quantification* (K.F.J. Heinrich & D.E. Newbury, eds.). Plenum Press, New York, N.Y. (31-75).
- SEBAI, A., FERAUD, G., BERTRAND, H. & HANES, J. (1991):  $^{40}\text{Ar}/^{39}\text{Ar}$  dating and geochemistry of tholeiitic magmatism related to the opening of the Central Atlantic rift. *Earth Planet. Sci. Lett.* 104, 455-472.
- SEMELEV, Y.E.I. (1994): Minerals and ores of the Khibiny-Lovozero alkali massif. *Geochem. Int.* 31(3), 160-165.
- SHEARER, C.K. & LARSEN, L.M. (1994): Sector-zoned aegirine from the Ilfmaussaq alkaline intrusion, South Greenland: implications for trace-element behavior in pyroxene. *Am. Mineral.* 79, 340-352.
- SØRENSEN, H. (1960): On the agpaitic rocks. *Int. Geol. Congress, 21st Sess. (Norden)* 13, 319-327.
- \_\_\_\_\_. (1974): Petrography and petrology of alkali syenites. In *The Alkaline Rocks* (H. Sørensen, ed.). John Wiley & Sons, London, U.K. (15-52).
- STEPHENSON, D. (1972): Alkali clinopyroxenes from nepheline syenites of the South Qôrøq centre, south Greenland. *Lithos* 5, 187-201.
- SYKES, L.R. (1978): Intraplate seismicity, reactivation of preexisting zones of weakness, alkaline magmatism, and other tectonism postdating continental fragmentation. *Rev. Geophys. Space Phys.* 16, 621-687.
- TYLER, R.C. & KING, B.C. (1967): The pyroxenes of the alkaline igneous complexes of eastern Uganda. *Mineral. Mag.* 36, 5-21.
- ULRICH, H.H.G.J. & GOMES, C.B. (1981): Alkaline rocks from continental Brazil. *Earth Sci. Rev.* 17, 135-154.
- UPTON, B.G. (1974): The alkaline province of South-West Greenland. In *The Alkaline Rocks* (H. Sørensen, ed.). J. Wiley & Sons, London, U.K. (221-238).
- VILLENEUVE, M. (1984): *Etude géologique sur la bordure sud-ouest du craton ouest-africain. La suture panafricaine et l'évolution des bassins sédimentaires protérozoïques et paléozoïques de la marge nord-ouest du continent de Gondwana*. Thèse de doctorat, Univ. d'Aix-Marseille III, Marseilles, France.
- VLASOV, K.A., KUZ'MENKO, M.Z. & ES'KOVA (1966): *The Lovozero Alkali Massif*. Oliver and Boyd, Edinburgh, U.K.
- WILLIAMSON, J.H. (1968): Least square fitting of a straight line. *Can. J. Phys.* 46, 1845-1847.
- WILSON, M. & GUIRAUD, R. (1992): Magmatism and rifting in western and central Africa, from Late Jurassic to Recent times. *Tectonophys.* 213, 203-225.

*Received September 13, 1994, revised manuscript accepted August 14, 1995.*